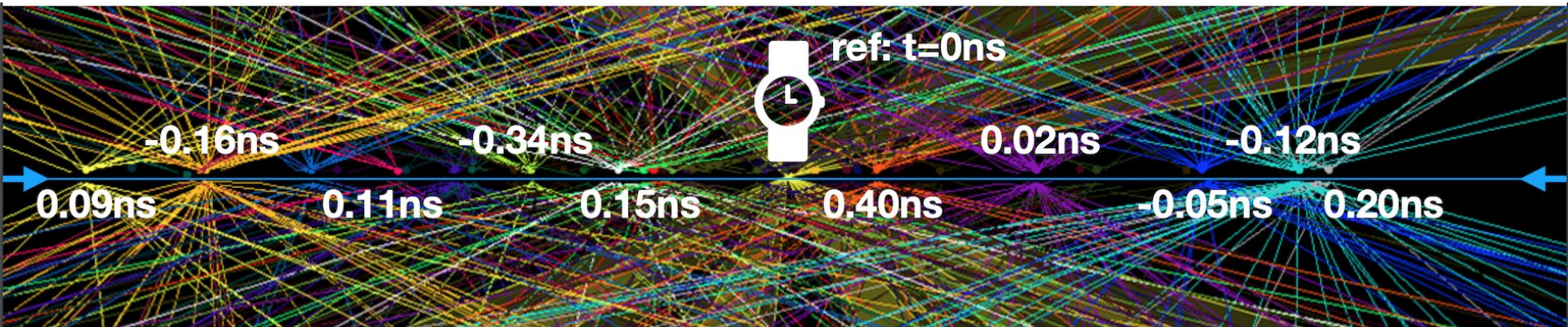


MIP Timing detectors at the LHC

Martina Malberti
(INFN Milano Bicocca)



- Introduction: why do we need precision timing detectors?
- Key concepts in timing measurements
- Precision timing detectors at the High Luminosity LHC
 - Silicon detectors (Low Gain Avalanche Diodes): CMS MTD Endcap Timing Layer, ATLAS HGTD
 - Light detectors (LYSO + SiPM): the CMS Barrel Timing Layer
- System aspects
- Timing applications in future colliders

Motivations for precision timing

Why precision timing?

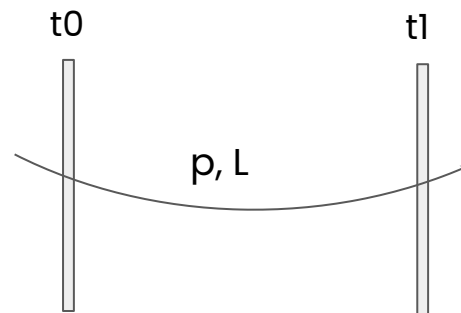
- Traditionally, **timing detectors used in HEP** to
 - trigger events
 - [particle identification through time-of-flight](#)
 - background suppression (rejection of non-beam events)
- Other well known **applications in other fields**
 - medical imaging ([TOF-PET](#))
- **New precision timing application in HEP**
 - [4D event reconstruction at colliders \(HL-LHC\)](#) to reduce background from concurrent collisions per beam crossing

Time-of-flight for particle identification

- Simple principle
- Measure **difference in time of arrival** of particles at two planes $t = t_1 - t_0 \rightarrow$ velocity $\beta = L/ct$
- Combined with a measurement of its **momentum** p , the mass of the particle can be calculated

$$p = m \gamma \beta c$$

$$m = \frac{p}{\gamma \beta c} = \frac{p}{c} \sqrt{\frac{c^2 t^2}{L^2} - 1}$$



TOF for PID: the need for good time resolution

- Mass resolution

$$\left(\frac{\delta m}{m}\right)^2 = \left(\frac{\delta p}{p}\right)^2 + \left(\gamma^2 \frac{\delta L}{L}\right)^2 + \left(\gamma^2 \frac{\delta t}{t}\right)^2$$

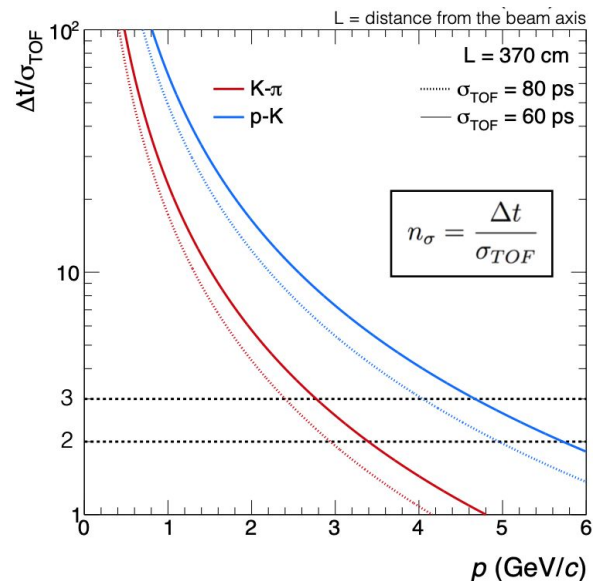
- $\delta p/p$ and path length uncertainties usually small
- mass resolution dominated by $\delta t/t$

- Mass separation

$$\Delta t = \frac{L}{\beta_1 c} - \frac{L}{\beta_2 c} = \frac{L}{c} \left(\sqrt{1 + \frac{m_1^2}{p^2}} - \sqrt{1 + \frac{m_2^2}{p^2}} \right)$$

$$\Delta t \sim \frac{Lc}{2p^2} (m_1^2 - m_2^2) \quad \text{for relativistic particles } p^2 \gg m^2 c^2$$

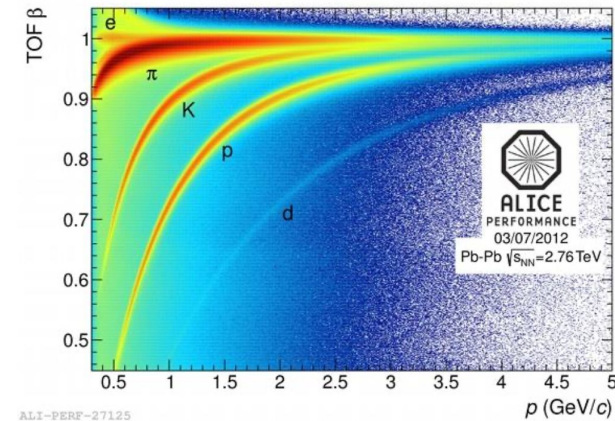
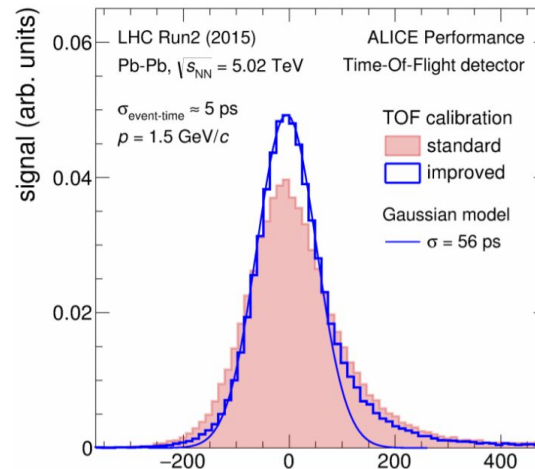
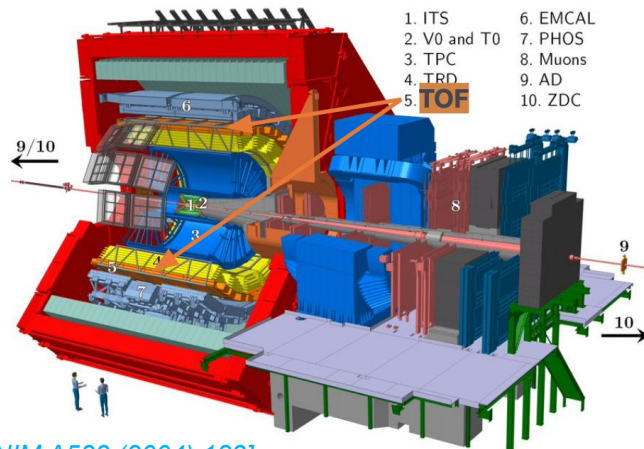
- for a given time resolution the path length needed to separate two particle types increases quadratically with p
- mass separation power decreases at high momentum, for fixed L



Good time resolution is essential

State-of-the-art TOF at colliders

- **ALICE TOF at the Large Hadron Collider** (in operation)
 - particle identification with Multigap RPCs (140 m² active area) at 3.7 m from the interaction point (IP)
 - provides charged-particle PID in the intermediate momentum range
 - TOF relative to the IP time (event time) defined using high multiplicity of tracks: $\Delta t = t_{\text{TOF}} - t_{\text{IP}}$
- **Single particle resolution $\sigma_{\text{TOF}} \sim 60$ ps**
 - 40 ps with a single channel at test beam
 - $\oplus \sim 40$ ps of system effects from 10⁵ channels
 - channel pulse uniformity, cross-calibration, clock distribution, event time

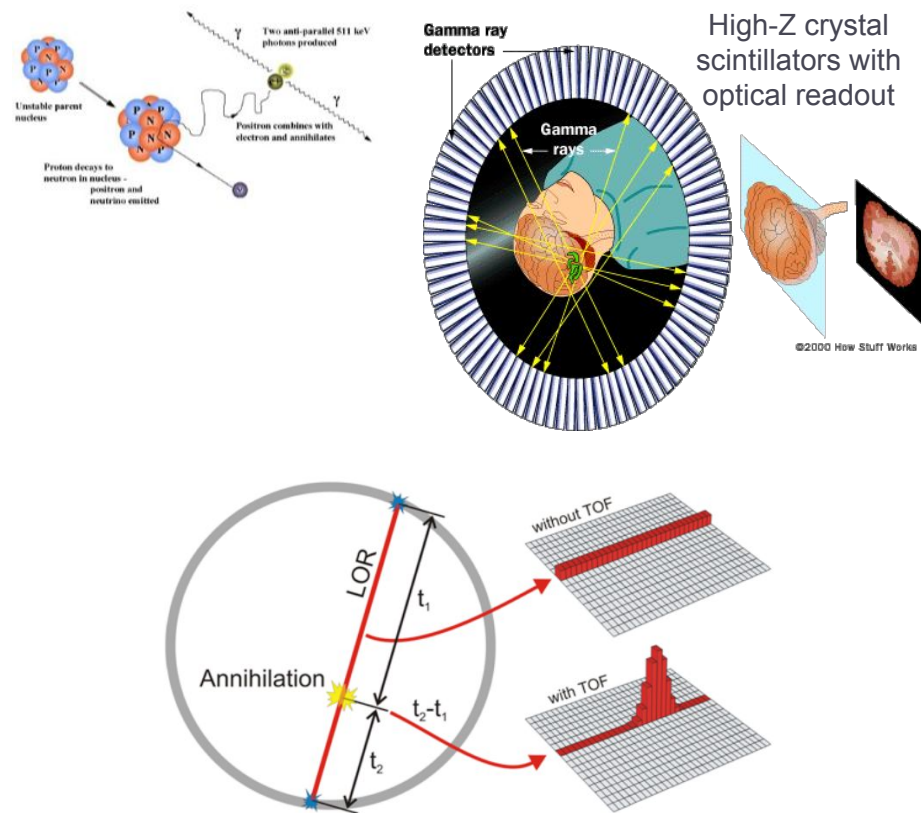


[NIM A533 \(2004\) 183\]](#)

[ALICE Coll.. PoS \(LHCP2018. 232\]](#)

Other time-of-flight applications: TOF-PET

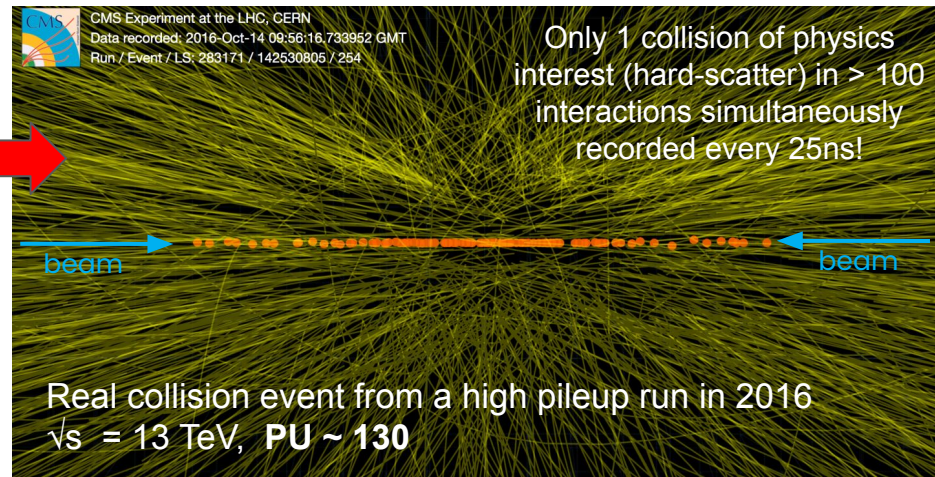
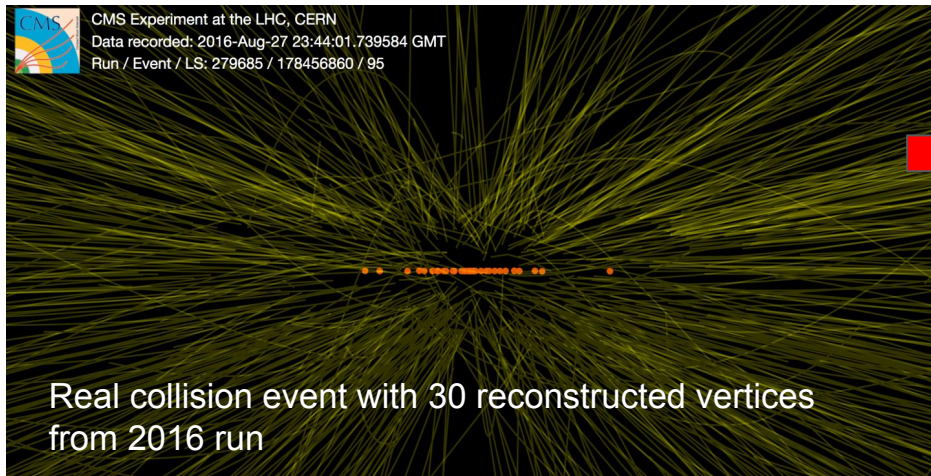
- Positron Emission Tomography (PET)
- Functional imaging that exploits the annihilation of β^+ emitted by a radiotracer with an electron in the tissue
- The image is reconstructed from intersection of lines of responses (LORs), formed by two 511 keV γ -rays detected in coincidence
 - signal: back-to-back γ -rays
 - background: fake LORs from scattered γ -rays, or accidental coincidences, reduce the image quality
- TOF-PET help reduce background restricting the search region to a few cm of the LOR
- State-of-the-art TOF-PET scanners achieve FWHM coincidence time resolutions of $O(100)$ ps



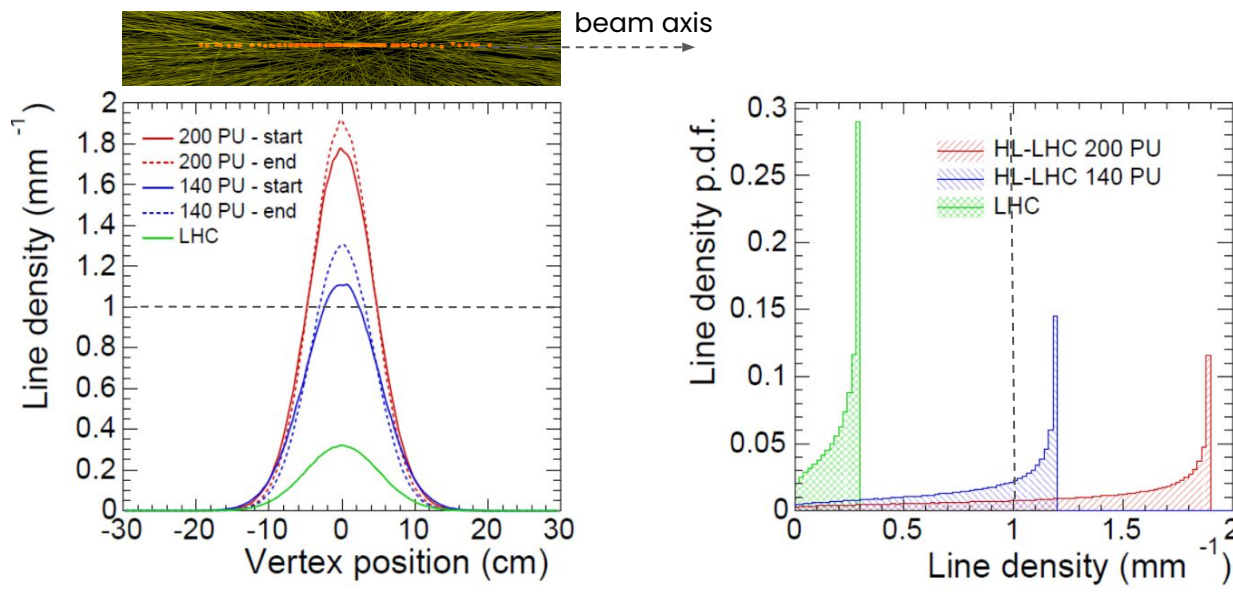
The High Luminosity LHC challenge

- High Luminosity LHC phase (2029–2042):
 - significant upgrade of optics and injectors to increase beam intensity
 - up to **200 simultaneous interactions** per beam crossing
- Need new detectors and methods needed to
 - keep current performance during the HL-LHC phase
 - cope with increased radiation damage

	Phase I LHC	HL-LHC
E_{beam} (TeV)	7-13.6	14
$\mathcal{L}_{\text{peak}}$ ($\text{cm}^{-2} \text{s}^{-1}$)	2×10^{34}	$5\text{-}7.5 \times 10^{34}$
$\int \mathcal{L}$ (fb^{-1})	300-500	3000-4000
Pileup (PU)	40-60	140-200



The High Luminosity LHC challenge



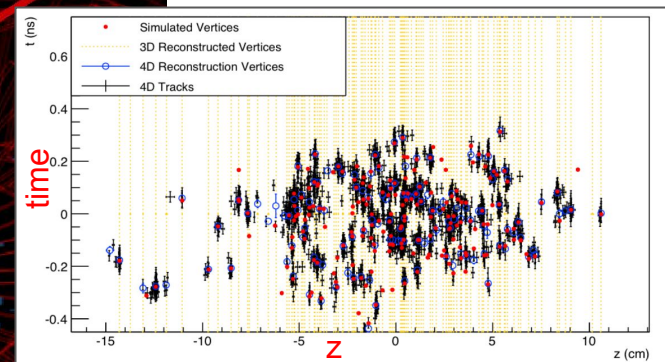
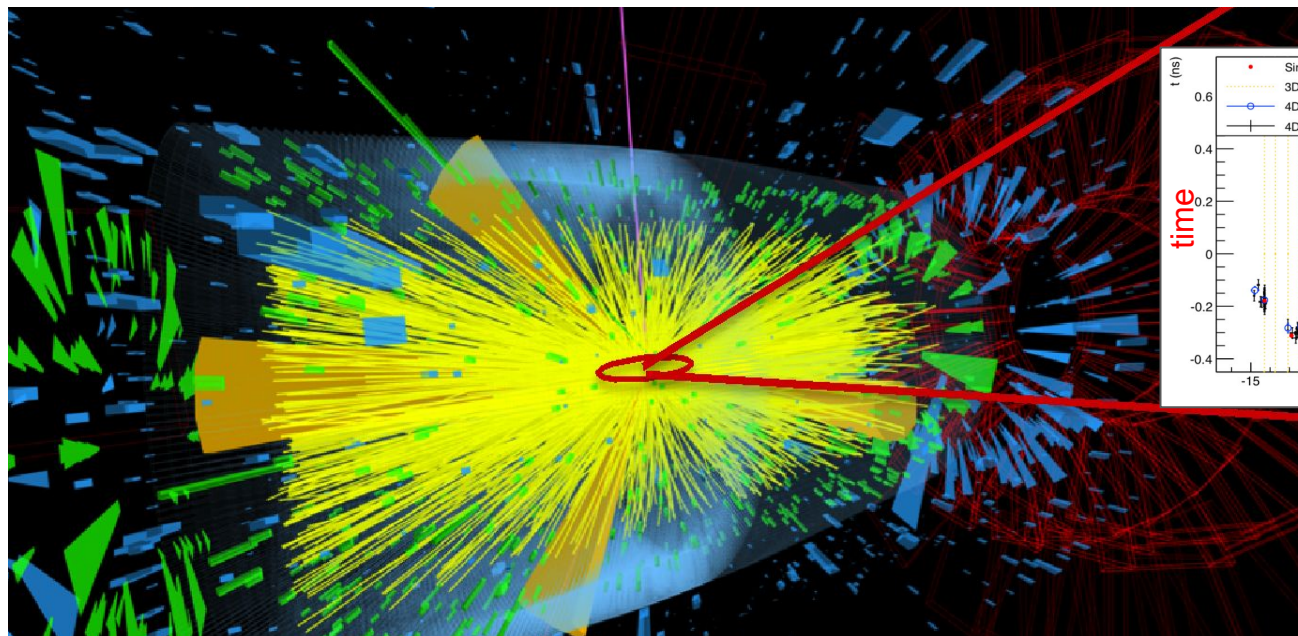
LHC → about 0.3 vertices /mm

HL-LHC → up to 1.9 vertices /mm

- Current global event reconstruction relies on track-vertex association in space
 - optimal for $|dz(\text{track}, \text{vertex})| \sim 1 \text{ mm}$
- This association becomes ambiguous when for event densities higher than 1 mm^{-1} (x6 wrt LHC)
 - large number of pileup tracks incorrectly assigned to the vertex of interest
 - degradation in most event observables: vertex merging, final state kinematics distorted, final state objects (jets, leptons, photons) identification affected

Precision timing for pileup mitigation

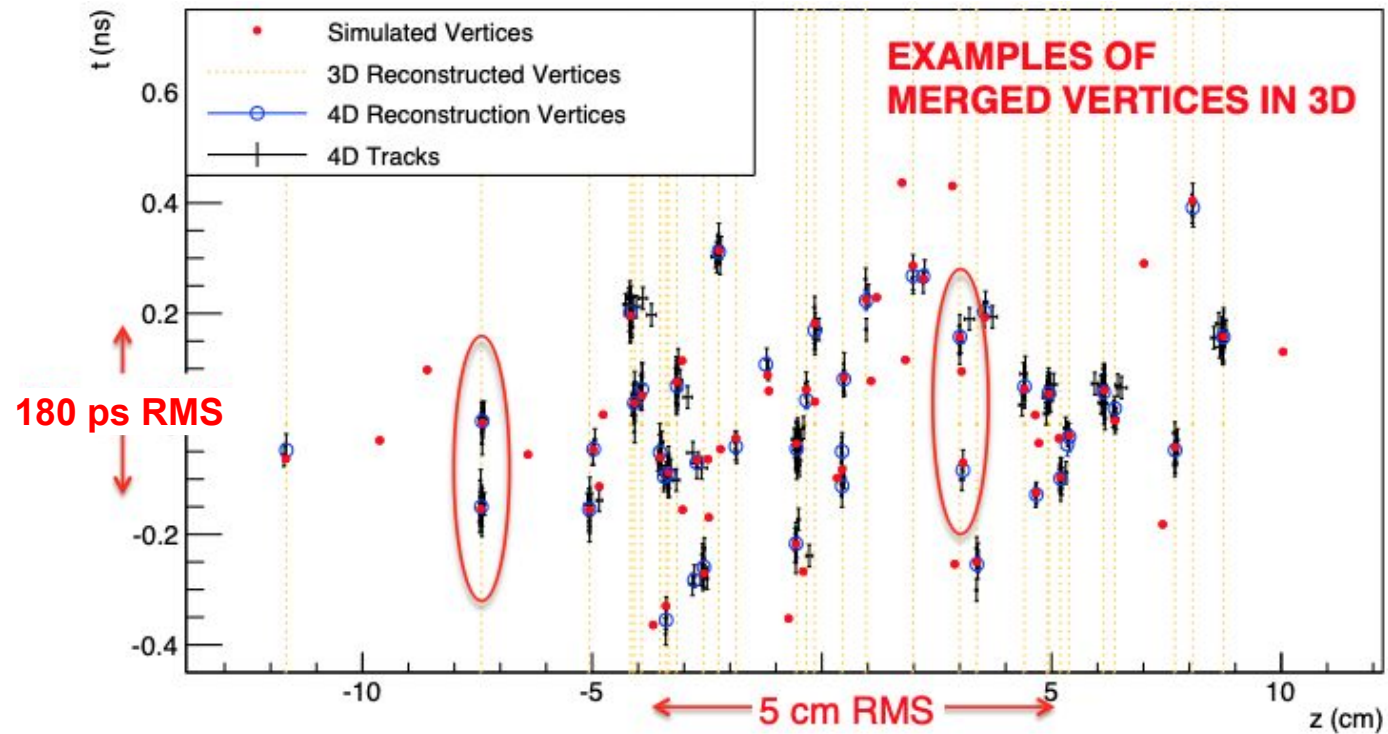
- Spread of the interactions in time **~ 180 ps (RMS)**
→ **exploit the time dimension of the beam spot for pileup mitigation**
- If the beam-spot is “sliced” in successive $O(30)$ ps time exposures, the effective pileup would be reduced by a factor 4-5



Luminous region
• t RMS ~ 180 ps
• z RMS ~ 5 cm

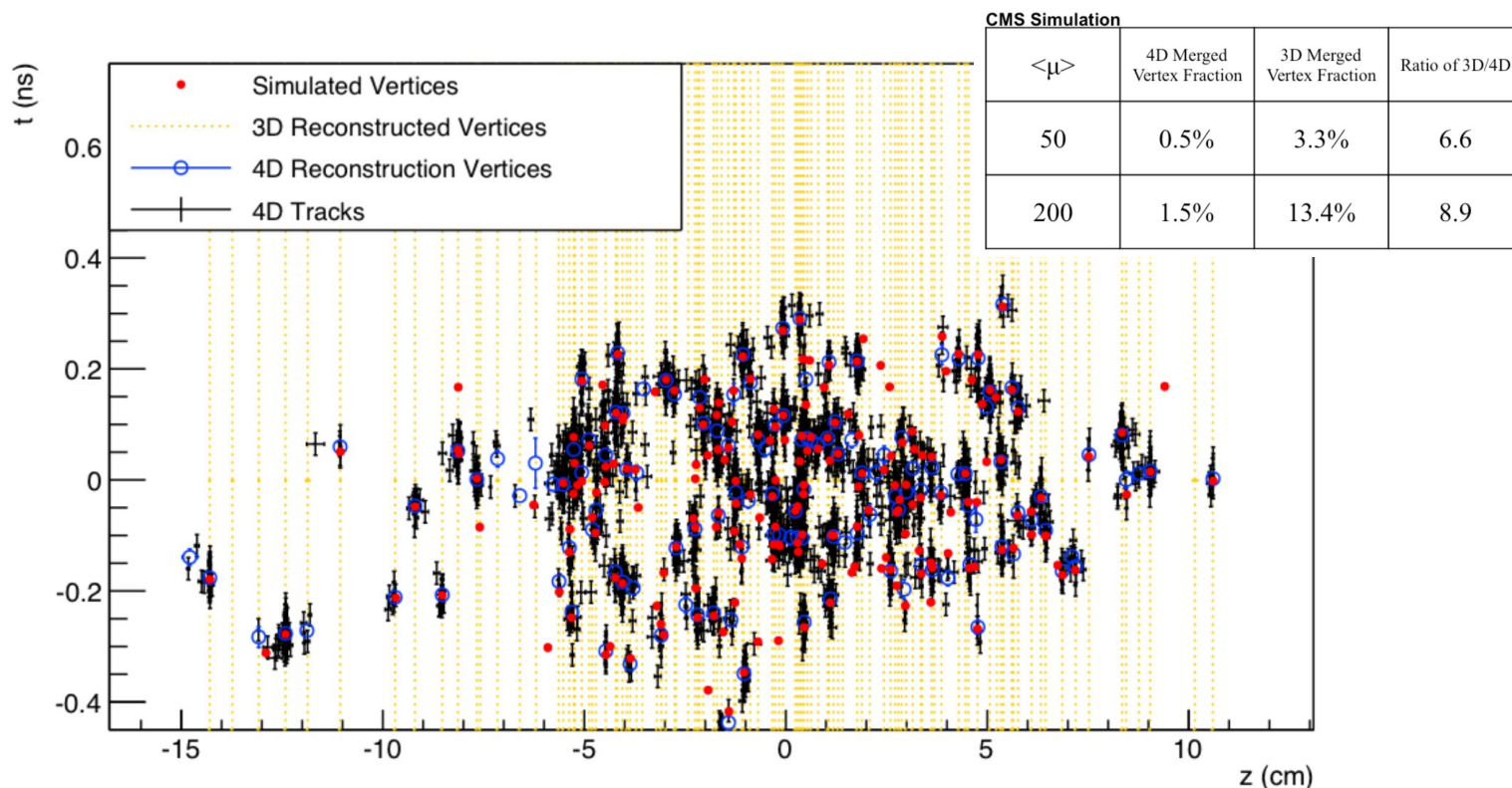
3D vs 4D vertex reconstruction

Example event display with PU = 50 (to ease eye analysis)



- 4D vertex reconstruction with track time information at ~ 30 ps
- Spatially overlapping vertices resolved in the time dimension

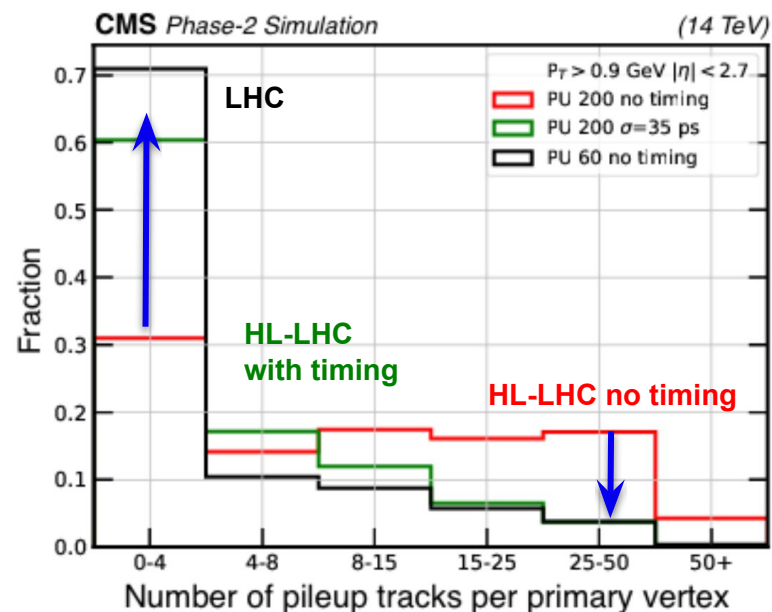
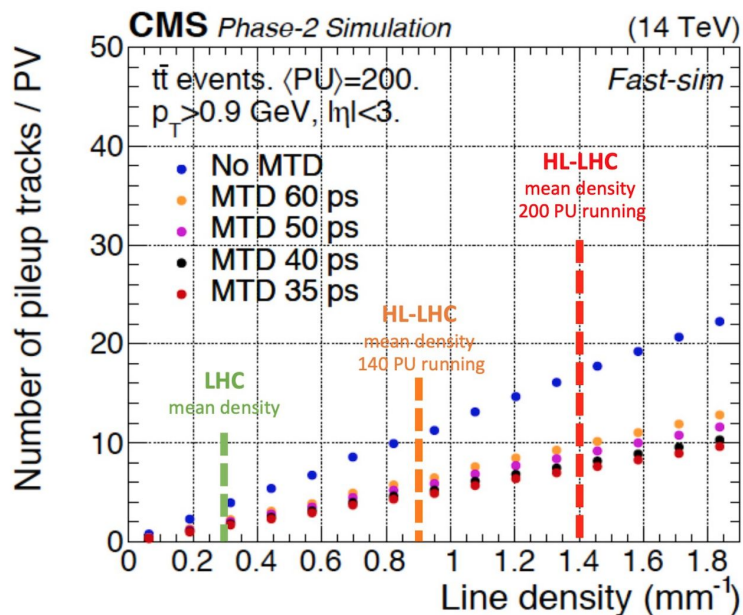
3D vs 4D vertex reconstruction – pileup = 200



- **4D vertex reconstruction with track time information at ~ 30 ps**
- **Spatially overlapping vertices resolved in the time dimension**

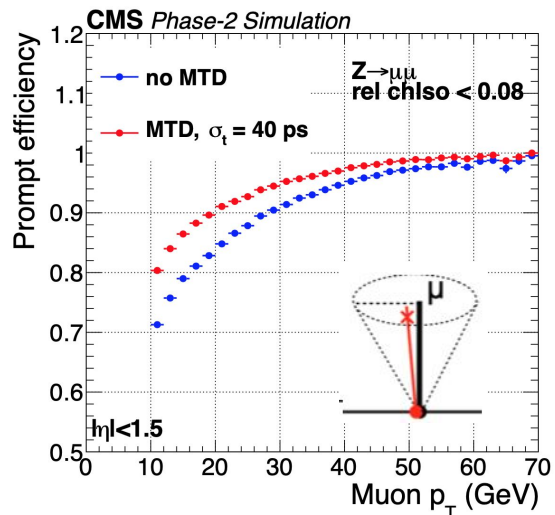
3D vs 4D vertex reconstruction

- Time-aware primary vertex reconstruction
 - reduces incorrect association of tracks from nearby pileup interactions by a factor of 2:
 - fully offsets the impact of the transition from 140 to 200 PU running
 - brings per-vertex track purity close to typical current LHC running conditions

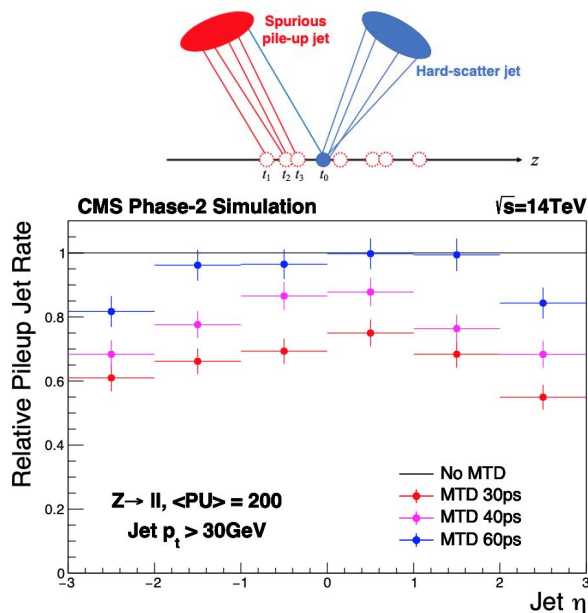


Physics impact: object reconstruction

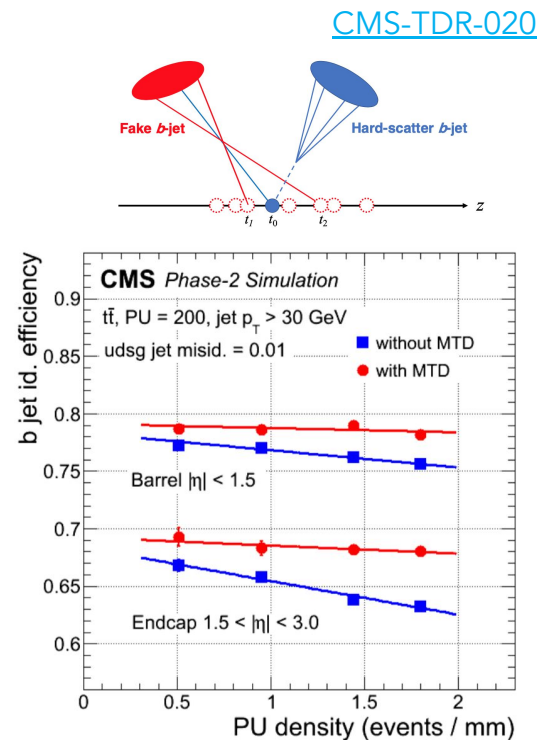
- Removal of PU tracks inconsistent with the hard interaction improves the quality of physics objects reconstruction and selection at the HL-LHC:
 - improved b-tagging, lepton isolation, photon identification
 - better rejection of fake jets due to pile-up
 - improved missing transverse momentum resolution



Increased lepton isolation efficiency

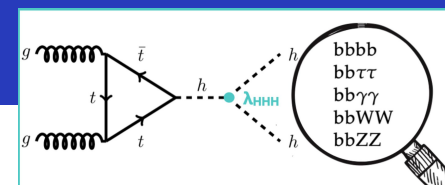


Reduction of fake jets



Improved b-tagging

Physics impact: HH searches



- HH searches at the HL-LHC
- Gains on single final-state particles compound in multi-object final states
 - 10%–20% gain in s/\sqrt{b} for many Higgs decay channels
- These improvements w/o MTD would require ~20–30% more luminosity (+2–3 years of data taking)

HH production sensitivity (sigmas) at 3 ab^{-1}

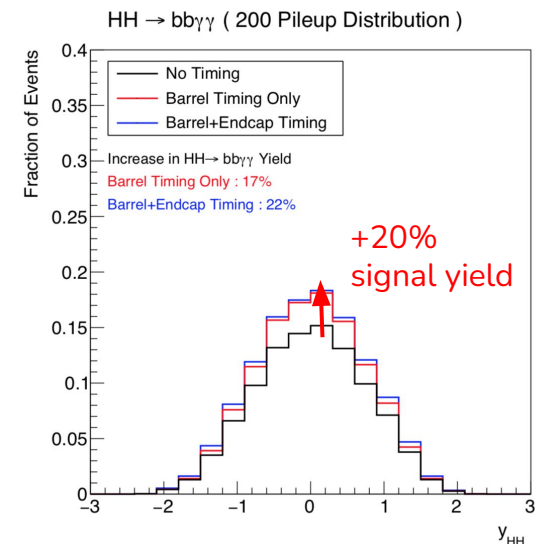
Channel	35 ps BTL, 35 ps ETL			
	No MTD	ETL Only	BTL Only	MTD
$bbbb$	0.88	0.90	0.93	0.95
$bb\tau\tau$	1.30	1.38	1.52	1.60
$bb\gamma\gamma$	1.70	1.75	1.85	1.90
Combined	2.31	2.40	2.57	2.66
+bbWW, bbZZ				2.75

Channel	50 ps BTL, 50 ps ETL			
	No MTD	ETL Only	BTL Only	MTD
$bbbb$	0.88	0.90	0.93	0.95
$bb\tau\tau$	1.30	1.36	1.44	1.50
$bb\gamma\gamma$	1.70	1.72	1.78	1.80
Combined	2.31	2.37	2.47	2.53
+bbWW, bbZZ				2.63

CMS projections for HH signal significance without and with timing

35 ps - nominal MTD TDR scenario
50 ps - scenario with potential degraded performance due to radiation damage

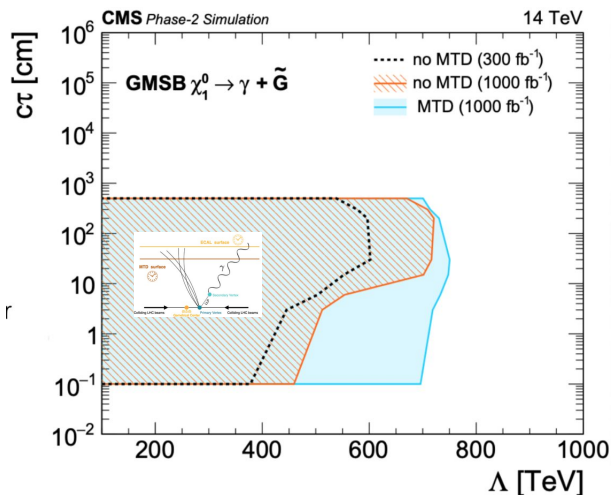
[CMS-DP-2022-025](#)



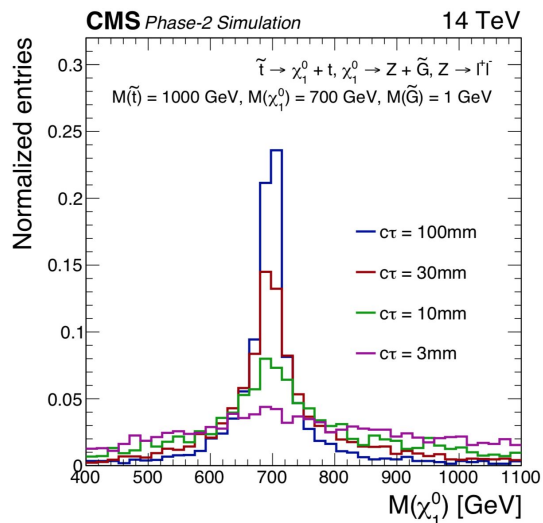
Measurement of the HH production and determination of the Higgs self-coupling is one of the main goals of the HL-LHC physics program

Physics impact: adding new capabilities

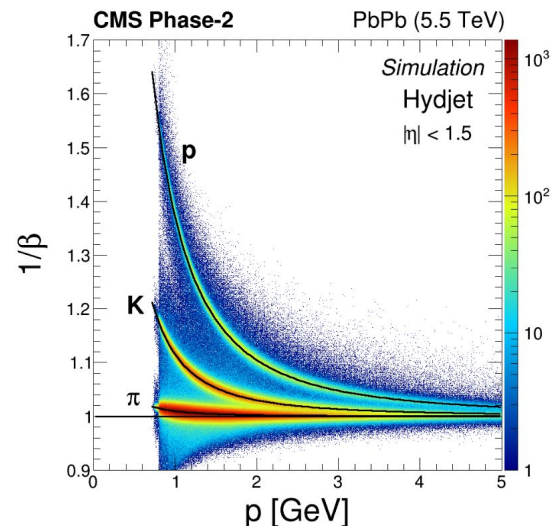
- Extend the sensitivity to BSM long lived particles beyond typical analysis strategies
- TOF resolution provides particle identification (PID) capabilities



*LLP decaying to delayed photons:
 → Timing detector essential to determine the primary vertex time
 → improved sensitivity with $\Delta t(vtx, \gamma)$*



Potential for direct measurement of LLP mass by reconstruction of the time of displaced vertices

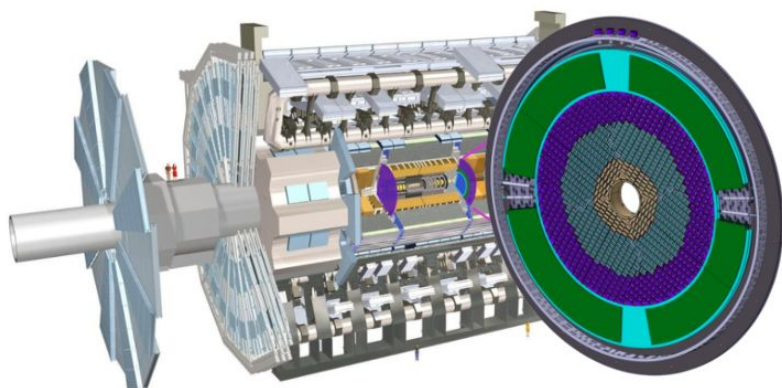


*PID of low momentum charged hadrons through TOF measurement
 → benefits to Heavy Ions and B-physics*

$$\Delta t = \frac{L}{c} \left(\frac{1}{\beta_{meas}} - \frac{1}{\beta_{hyp}} \right)$$

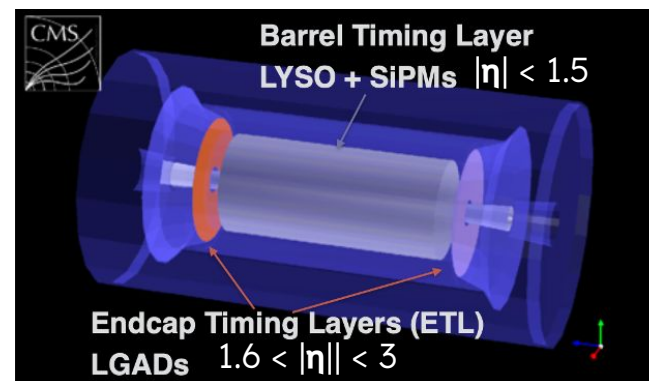
ATLAS High Granularity Timing Detector

- forward region $2.4 < |\eta| < 4.0$
- 2 double instrumented disks of Low Gain Avalanche Diodes (**LGADs**) at $z = \pm 3.5$ m from IP
- $\sigma_t \sim 30\text{--}50$ ps per track



CMS MIP Timing Detector

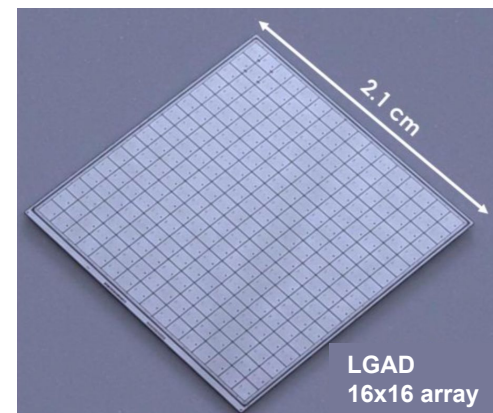
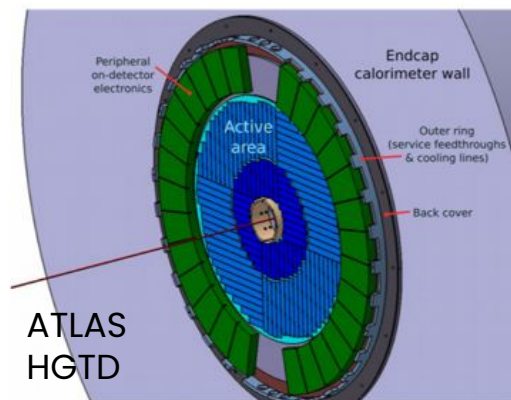
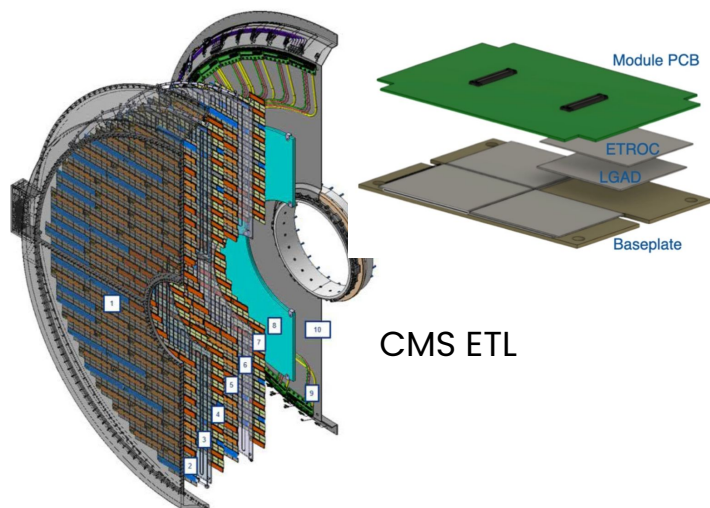
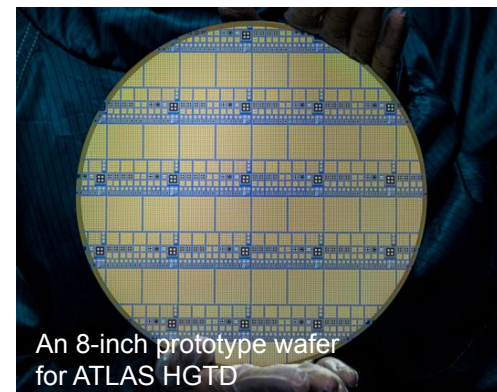
- **BTL**: single layer **LYSO+SiPM** readout at $R = 1.1$ m
- **ETL**: Two disks of **LGADs** per end ($z = \pm 3$ m)
- $\sigma_t \sim 30\text{--}40$ ps at start up, **BTL degrades to 50–60 ps** at end of HL-LHC (radiation damage)



- Cost-effective coverage of large areas
 - Mechanics, services and schedule compatible with existing upgrades
 - Minimal impact on calorimeter and tracker performance
 - Rate capability and radiation tolerance
 - **Radiation $\sim 10\times$ LHC**: 2×10^{14} (Barrel), up to 2×10^{15} (CMS endcaps) and $2.5 \times 10^{15} n_{eq}/\text{cm}^2$ (ATLAS)

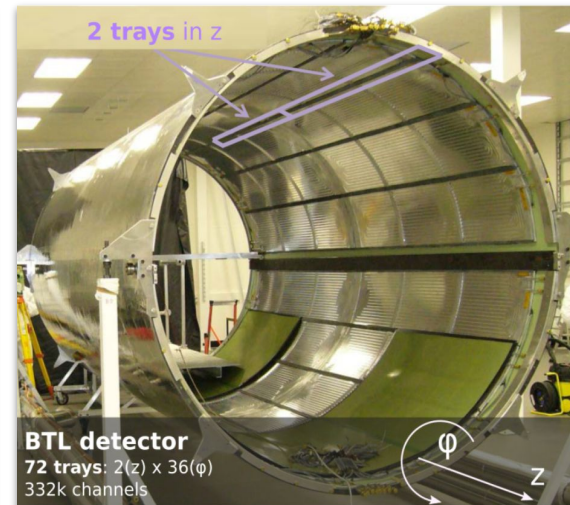
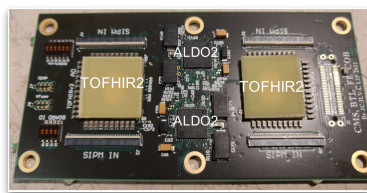
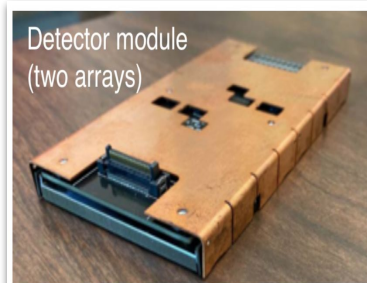
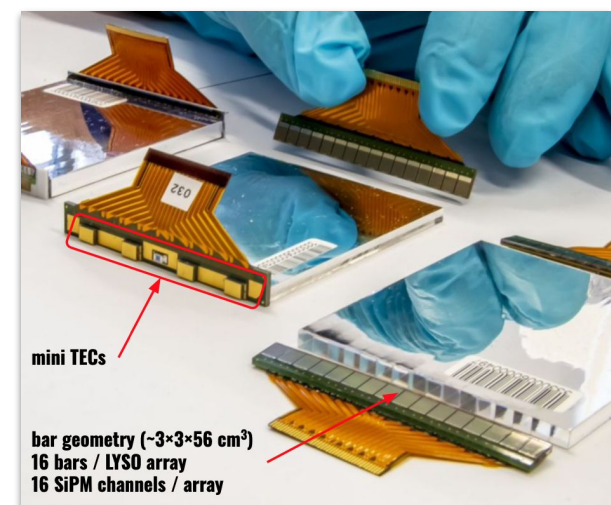
Overview: LGAD arrays for CMS ETL / ATLAS HGTD

- 16 x 16 (ATLAS 15 x 15) pads of $1.3 \times 1.3 \text{ mm}^2$ pixels
- $50 \mu\text{m}$ thickness, bump bonded to the readout ASIC
- 3.5/8. MChannels in ATLAS/CMS
- surface 6.4 (ATLAS) / 14 (CMS) m^2 , including multiple layers
- Low temperature operation ($T = -30 \text{ }^\circ\text{C}$) with CO_2 dual-phase cooling
- Power consumption $\sim 5 \text{ kW/ m}^2$



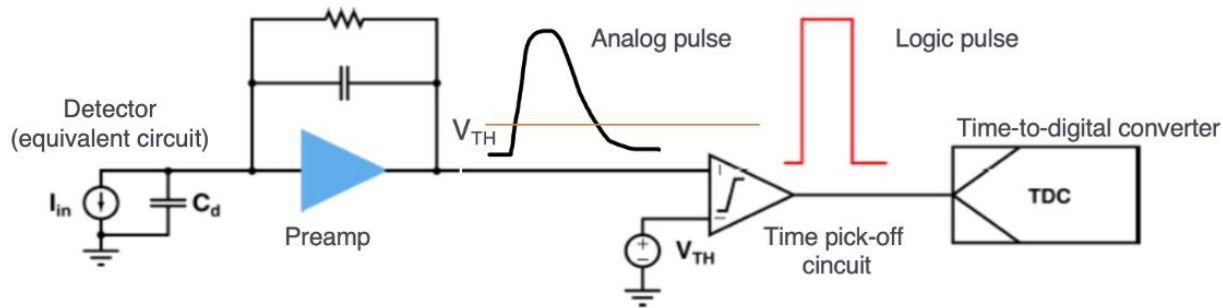
Overview: LYSO+SiPMs for the CMS Barrel Timing Layer

- Fundamental unit: array of 16 **LYSO:Ce bars** ($\sim 3 \times 3 \times 55 \text{ cm}^3$) read out by an array of 16 SiPMs on each side
- Thermo-electric coolers (TECs) integrated on the SiPM package
- ~ 10000 modules ($\sim 165\text{k}$ crystals, 332k channels) arranged in 72 mechanical units (trays)
- Total surface $\sim 38 \text{ m}^2$, SiPM surface $\sim 2 \text{ m}^2$
- Dedicated readout chip TOFHIR (110 nm technology)
- Low temperature operation ($T = -45^\circ\text{C}$) with CO_2 cooling + additional local cooling from TECs
- Power need $\sim 1\text{kW}/\text{m}^2$



Key concepts in timing measurements

Time measurements



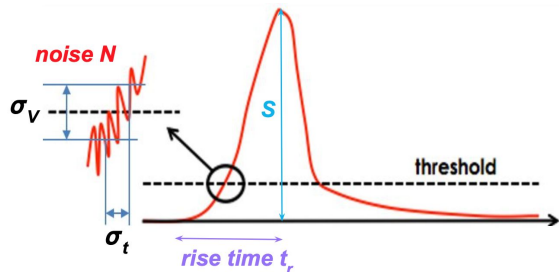
- Time measurement
 - the current signal from the sensor is amplified and shaped
 - time pick-off: a comparator generates a logic pulse whose leading edge indicates the time of occurrence of the input analog pulse
 - digitization: the time of the logic pulse (relative to a clock) is digitized by a time-to-digital converter (TDC)
- The time resolution depends on:
 - pulse properties at the input of the time pick-off device (combination of detector and shaping properties)
 - the time pick-off method
 - leading edge discrimination with a threshold comparator most popular in ASICs
 - the digitization step (subleading)
- Strong interplay between sensors and electronics
 - rule of thumb: the spread on a small time-interval is small, i.e., keep the charge generation localized and have fast signals (short time collection and fast pulse shaping)

Time resolution terms

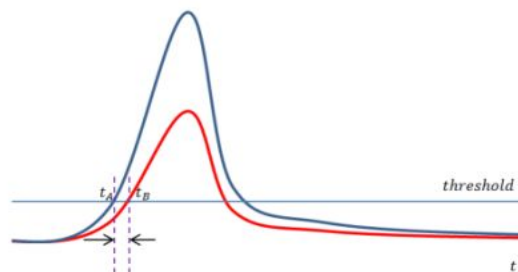
- The time resolution of a detector can be expressed as the sum of different contributors which depend on the detector type and on the electronics

$$\sigma_t^2 = \sigma_{jitter}^2 + \sigma_{ioniz.}^2 + \sigma_{TDC}^2 + \sigma_{clock}^2$$

Time jitter:
inaccuracy due to noise



Fluctuations in signal formation from ionization process and uniformity of charge collection
→ time walk



Subleading terms (with proper design):

$$\sigma_{TDC} = \Delta TDC / \sqrt{12}$$

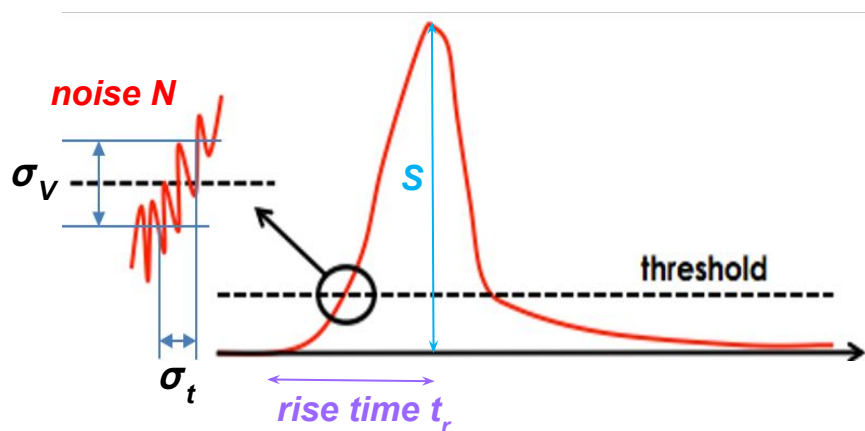
→ minimize TDC bin size

$$\sigma_{clock} < 15 \text{ ps}$$

→ specification for HL-LHC systems

Time jitter

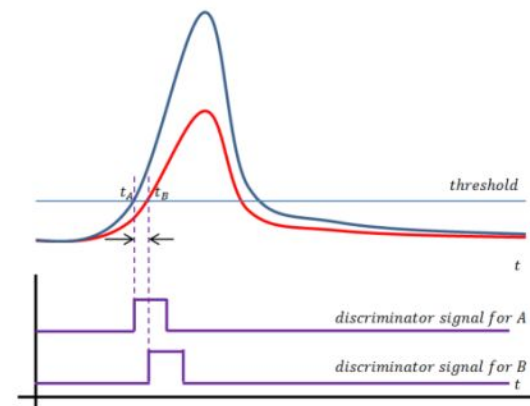
- The jitter term is due to the effect of the noise, N , when the signal is approaching the threshold, with a slope dV/dt
- Low jitter requires:
 - **high S/N** and **short rise time**
 - **wide readout bandwidth** matched to the signal risetime ($BW \sim 1/t_r$)



$$\sigma_t = \frac{\sigma_V}{\frac{dV}{dt}} = \frac{N}{S} = \frac{t_r}{S/N}$$

Time walk

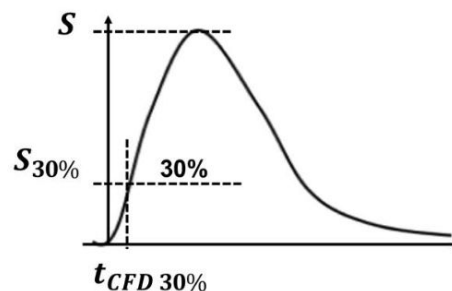
- **Signals of different amplitude cross a fixed threshold at different times**
- Shape variations can also cause the signal crossing the threshold at different times



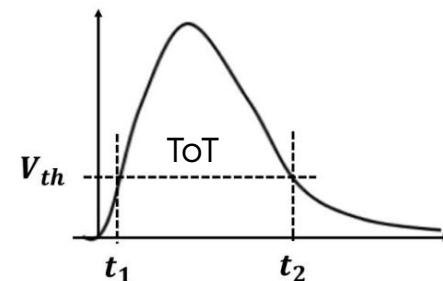
Time walk effect

Two usual solutions:

- 1) **constant fraction discriminator**: the time is set when a given fraction of the amplitude is reached
- 2) **correct (offline) using amplitude (S) or time-over-threshold (ToT)**



Constant Fraction Discriminator



Time-over-Threshold

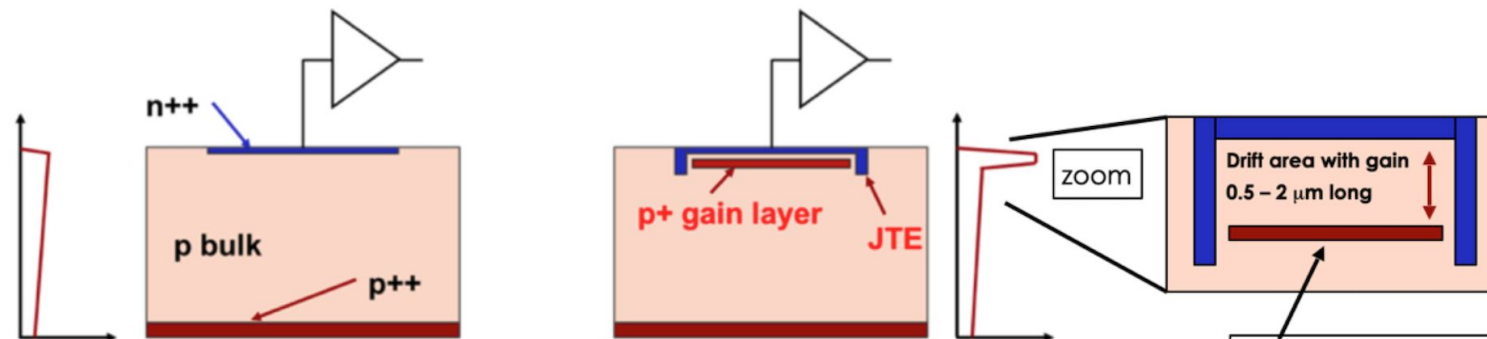
CMS BTL: time + integrated charge
CMS ETL and ATLAS HGDT: time + ToT

Timing with Low Gain Avalanche Diodes

- LGADs vs traditional Si diodes
- Signal formation in Si detectors
- Role of the gain and sensor thickness
- Time resolution performance
- Radiation tolerance

Reference: "An introduction to Ultra-Fast Silicon Detectors", <https://doi.org/10.1201/9781003131946>

Traditional Si diodes vs low gain avalanche diodes



E field Traditional Silicon detector

High value of the electric field obtained by applying external high bias voltage

Ultra fast Silicon detector E field

High value of the electric field in a localized region thanks to the additional p+ layer implanted near the PN junction

The gain layer:
a parallel plate capacitor with high field

Need $E > 300 \text{ kV/cm}$ for charge multiplication

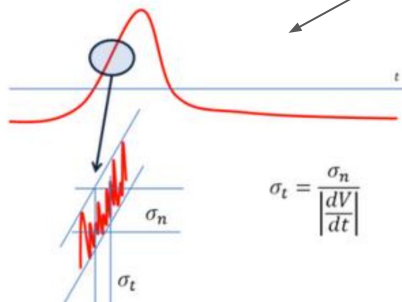
LGADS optimization for precision timing

- thin depletion region ($50 \mu\text{m}$) → uniform and fast signals
- internal gain (10-30) → enhances S/N

Time resolution terms

$$\sigma_t^2 = \sigma_{jitter}^2 + \sigma_{Landau}^2 + \sigma_{Distortion}^2 + \sigma_{TDC}^2$$

subdominant

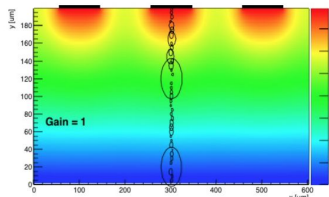
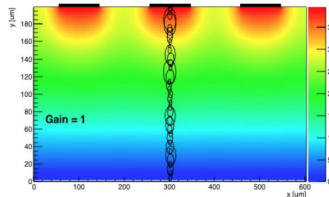


Small noise

→ optimize electronics

Large dV/dt

→ use sensors with internal gain

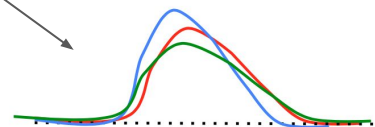


Amplitude variations

→ corrected offline (time walk)

Non-homogeneous energy deposition

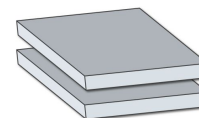
→ signal shape variations: cannot be corrected, to be minimized by design



Signal shape determined by Ramo's theorem

$$i = -q\vec{v}_d \cdot \vec{E}_w$$

Minimized by using **parallel plate geometry** and operating sensors at a bias voltage where the **drift velocity is saturated**



Signal formation – one e-h pair

- How signal is formed?
A charged particle crossing a sensor creates $e-h$ pairs.
The charge carrier's motion induces a variable charge on the read-out electrode.
The signal ends when all the charges are collected.

- Consider a simple case: Si diode, no internal gain, one electron-hole pair

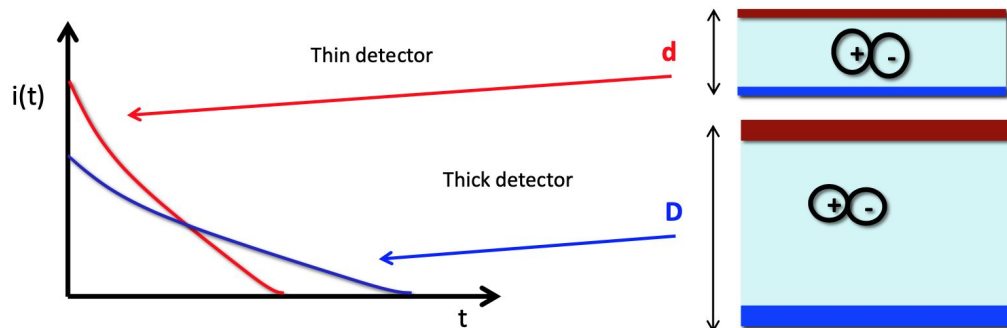
- $q = \text{integral of the induced current } \int [i_{el}(t) + i_h(t)] dt = q$

- For simple parallel plate capacitor geometry

$$i = q v_{drift} \frac{1}{d}$$

($1/d$ = weighting field for a parallel plate capacitor)

- One e/h pair generates higher current in thin detectors



(Simplified model for pad detectors)

Initial current and thickness

- Thick detectors have a large number of charges:

$$Q_{tot} = N_{e-h} q d$$

- Each charge contributes to the initial current as

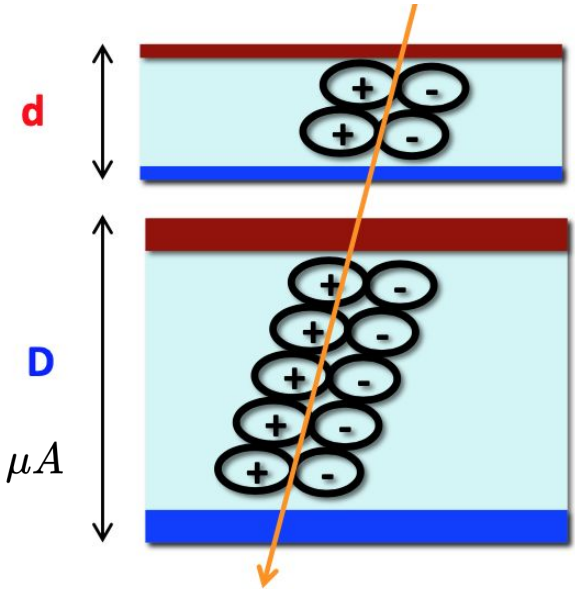
$$i = q v_{drift} \frac{1}{d}$$

- The initial current for a thick (d) detector is:

$$i = Q_{tot} v_{drift} \frac{1}{d} = (N_{e-h} q d) v_{drift} \frac{1}{d} \sim N_{e-h} q v_{drift} \sim 1 - 2 \mu A$$

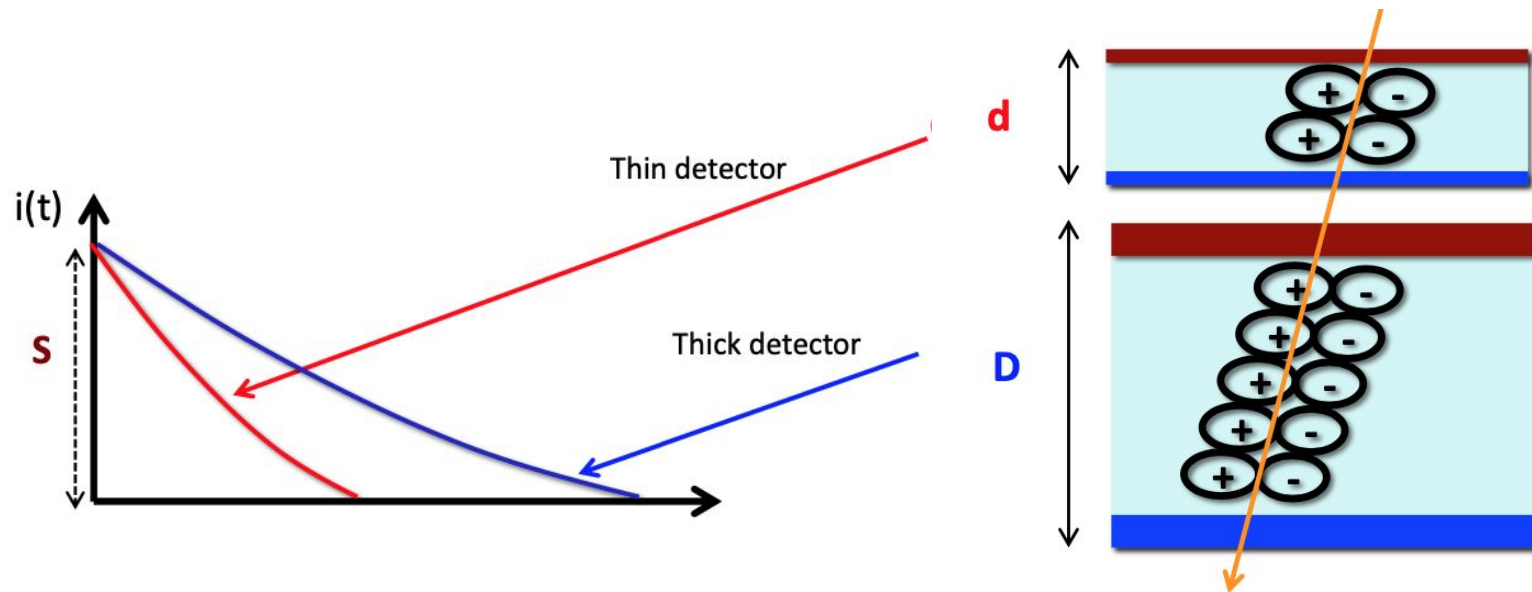
- The initial current doesn't depend on the thickness**
- Thickness affects the total charge and signal duration

ionization density in Si: $N_{e-h} \sim 75 \text{ e-h}/\mu\text{m}$
drift velocity $v_{drift} \sim 100 \mu\text{m/ns}$



(Simplified model for pad detectors)

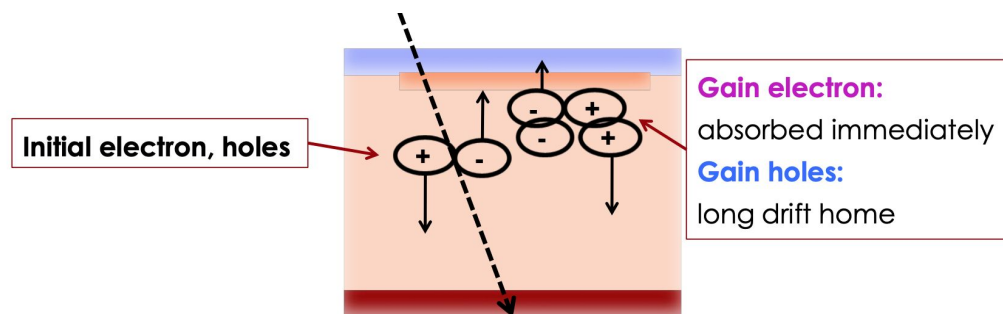
Initial current and thickness



- The initial current doesn't depend on the thickness
- Thickness affects the total charge and signal duration

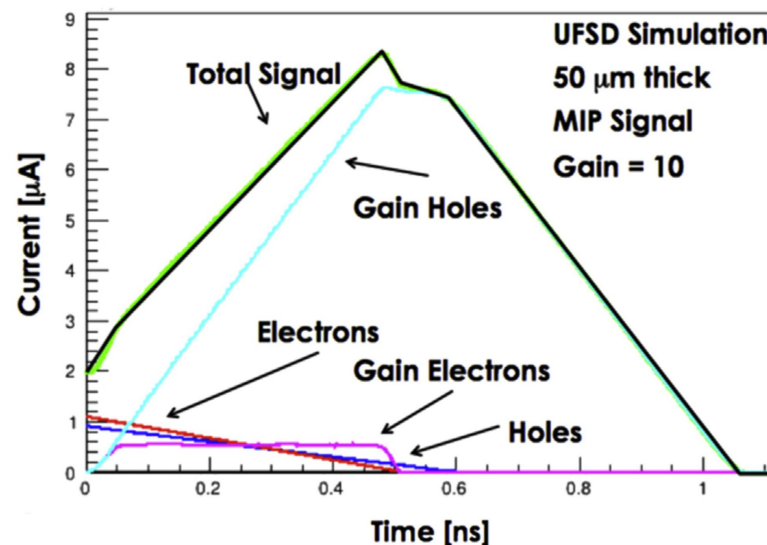
→ We need gain to boost the signal!

Signal formation in sensors with gain



How gain shapes the signal?

- Primary electrons enter the gain layer and start the avalanche multiplication mechanism, producing secondary e-h pairs
- gain electrons immediately collected by the cathode
- gain holes drift almost the full bulk thickness before being collected by the anode, generating most of the signal
- signal increases up to the collection of the last primary electron
- signal decreases to zero in an interval controlled by the holes drift velocity



Gain and detector thickness

- The current generated by the multiplication mechanism can be estimated from the number of electrons entering the gain layer in a time interval dt , assuming a drift velocity v_{sat}
- Number of secondary charges $dN_{gain} = N_{e-h} (v_{sat} dt) G$ $G = gain$
(the rate of production of secondaries is constant)
- **Current induced from secondary charges** (from Ramo's theorem):

$$dI_{gain} = q dN_{gain} v_{sat} \frac{1}{d} \propto \frac{G}{d} dt$$

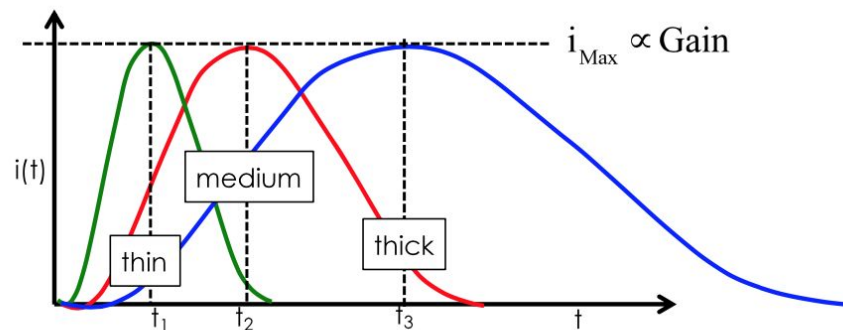
$$\frac{dI_{gain}}{dt} \sim \frac{dV}{dt} \propto \frac{G}{d} \rightarrow \text{thin sensor with gain to increase the SR}$$

- Since each primary electron generates G e-h pairs, the **maximum current** can be written as

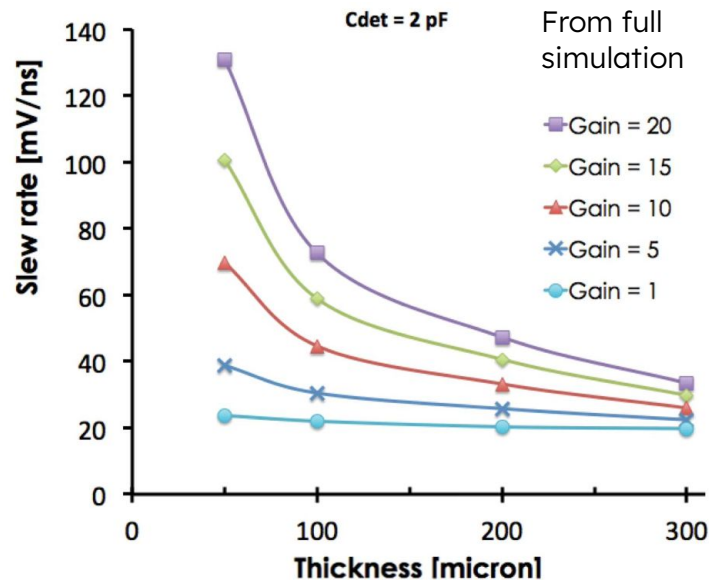
$$I_{max} = (N_{e-h} d G) q v_{sat} \frac{1}{d} \propto G$$

Gain and detector thickness

$$\frac{dV}{dt} \propto \frac{G}{d}$$



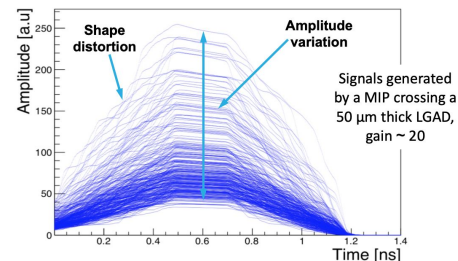
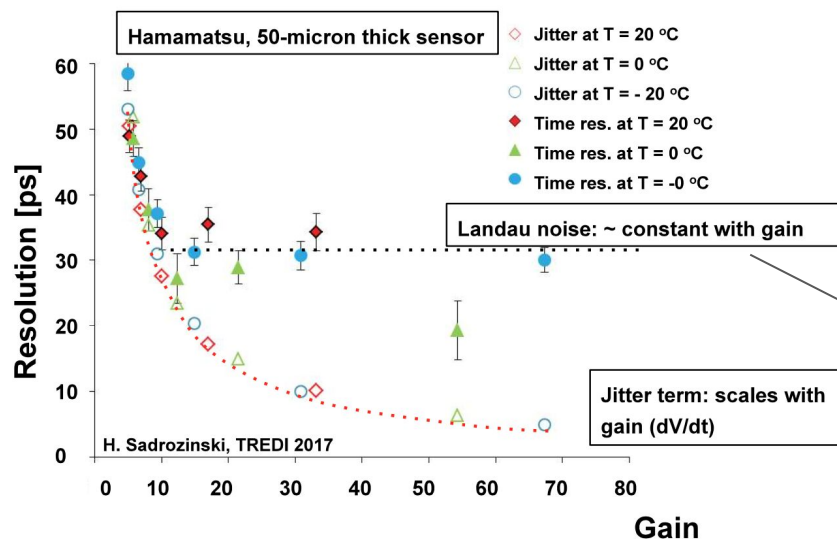
The rise time depends only on the sensor thickness $\sim d$



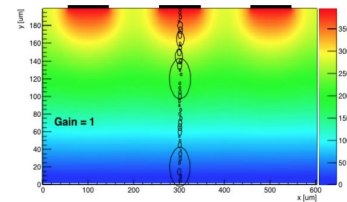
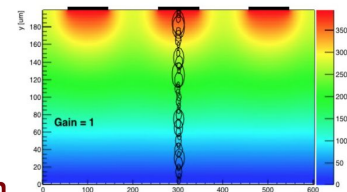
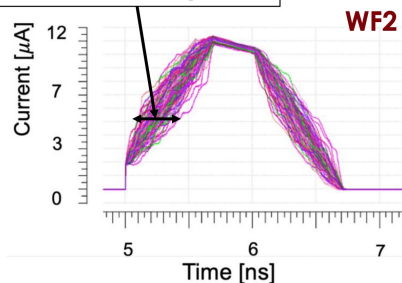
Significant improvements in time resolution require thin detectors with internal gain

Time resolution optimization

- **30 ps time resolution** can be achieved with LGAD sensors **50 μm thick, gain ~ 20**
- At lower gain, the jitter term dominates
- At large gain, time resolution plateaus at ≈ 30 ps due to fluctuations in the ionization process
 - Landau fluctuations \rightarrow the time spread of the primary current (σ_{ioniz}) grows with thickness

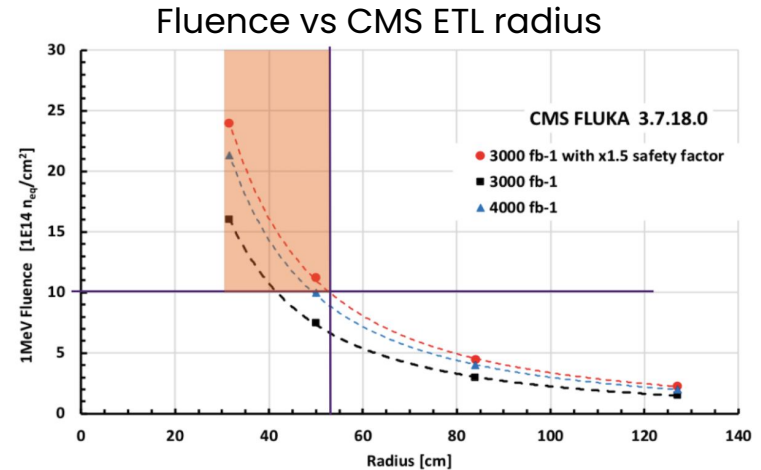
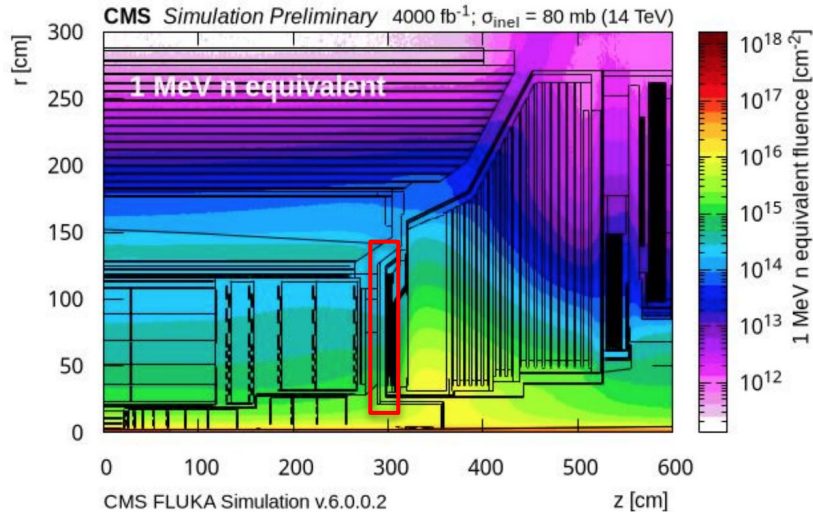


Intrinsic time spread



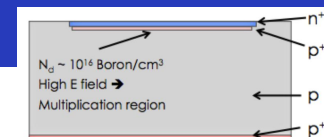
Irradiation effects in LGADs

- LGADs in CMS/ATLAS need to survive to **fluences up to $\sim 1.5\text{--}2.5 \times 10^{15} \text{ n}_{\text{eq}}/\text{cm}^2$**



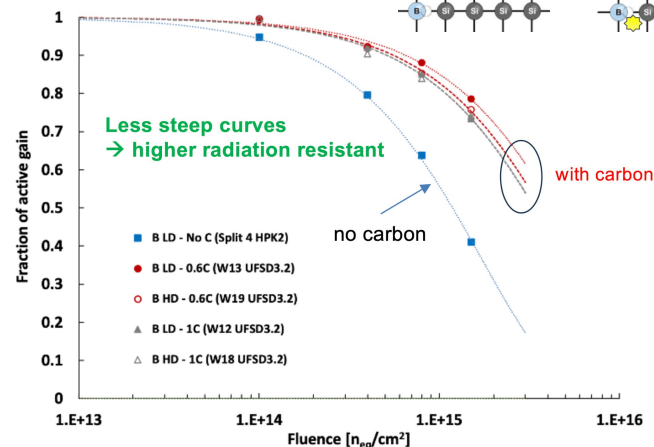
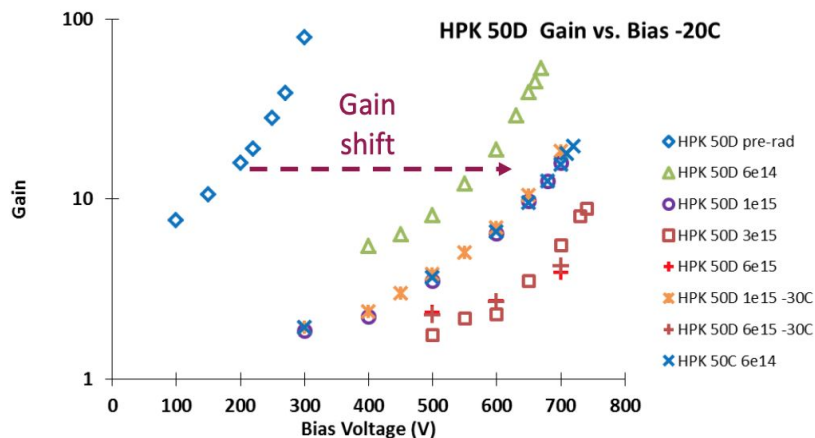
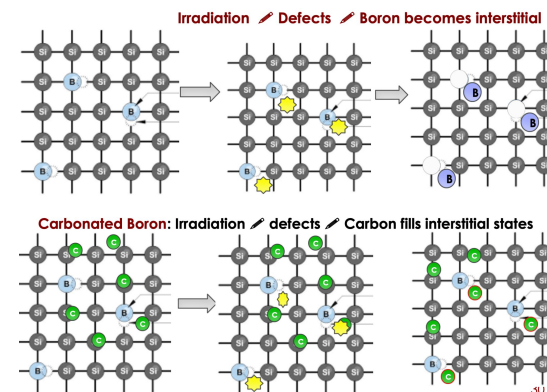
- Irradiation causes three main effects on LGADs:
 1. decrease of the charge collection efficiency due to trapping
 2. **variation in the doping concentration** (acceptor removal)
 3. increase in leakage current (mitigated with cooling at -30°C)

Radiation effects in LGADs : acceptor removal



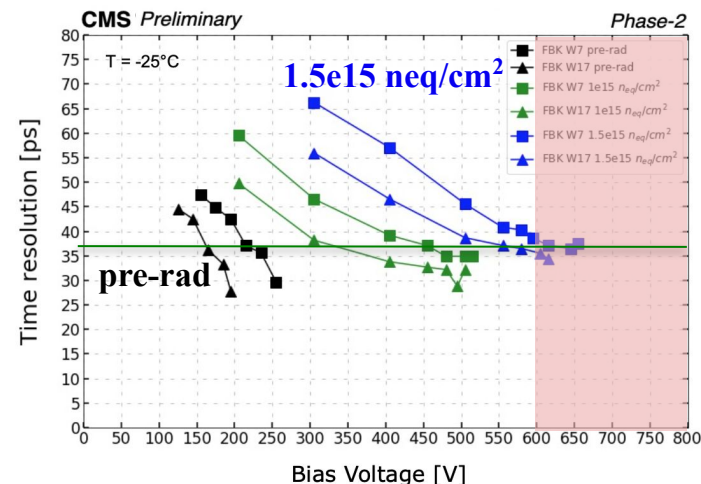
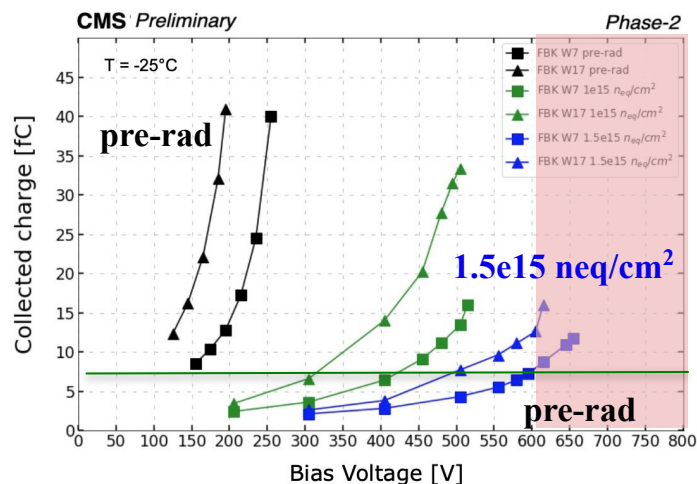
- The radiation deactivates p-doping removing Boron from the reticle, reducing the signal multiplication power of the LGAD sensors

- addition of Carbon or tuning of the doping profile can mitigate the effect
- increase bias voltage to maintain gain after irradiation



LGADs radiation tolerance

- Radiation tolerance tested in latest prototypes:
 - collected charge (>8 fC) and time resolution of the bare sensors is within requirements
 - **40 ps** resolution achieved for end of (CMS) operation
- Test beam studies show sparking damage to sensors above 600 V (120 kV/cm)
 - LGADs compatible with safe operation at HV < 600 V up to full fluence

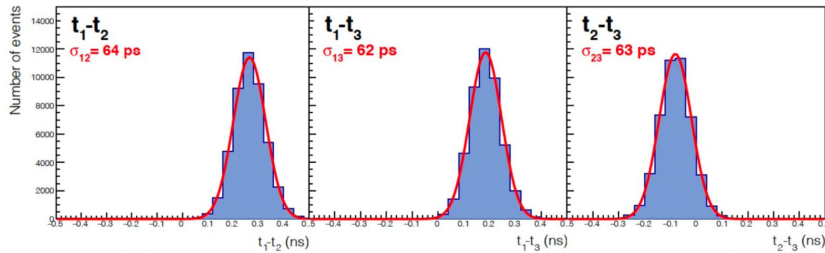
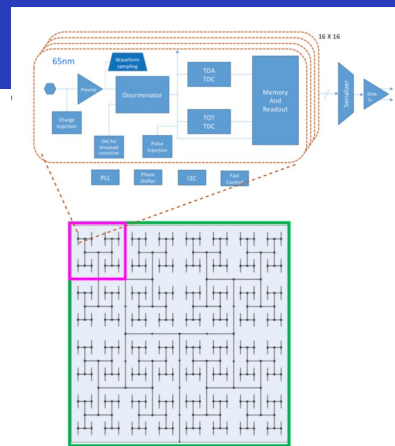


SEB – Single Event Burn out from rare, highly ionizing events

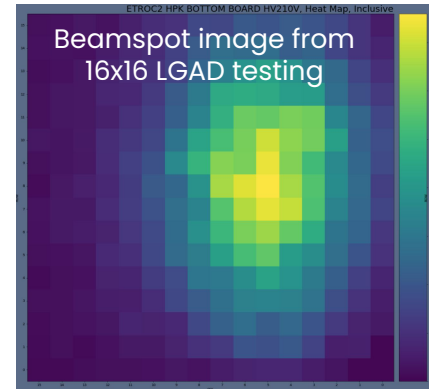
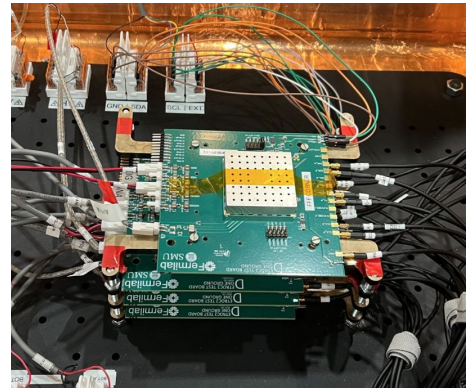
- An incoming particle releases a lot of energy over a small volume, 5-10 μm.
- The local electric field is high enough to create a conductive channel
- The energy stored in the sensor capacitance discharges burning the sensor

Performance validation

- Readout chip: ETROC (CMS), ALTIROC (ATLAS)
 - bump-bonded to LGAD, with 1.3 mm x 1.3 mm pads
 - requirement: ASIC contribution to time resolution < 40ps
 - deal with small signal size (~6fC, at end of operation)
 - low power consumption
- Test results with readout chip prototypes demonstrate the expected performance:
 - **~45 ps per hit**, matching specifications < 50 ps/hit and 30 ps/track with 2 hits/track



Preliminary test beam results with LGAD + ETROC1 (4x4) prototype: $\sigma_t = 42-46$ ps per hit



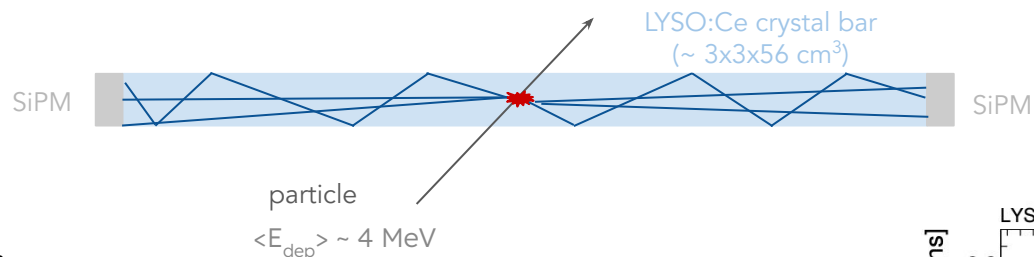
Ongoing tests with full size (16x16) chip

Timing with light detectors

- CMS barrel timing layer: principle of operation
- Time resolution drivers
- Solutions to deal with the SiPM dark noise
- Timing performance

Principle of detection

- **Particles traversing the crystal produce optical photons that are then detected by the SiPM**
- Signal discriminated by the ASIC to obtain the time at which the particle crossed the crystal



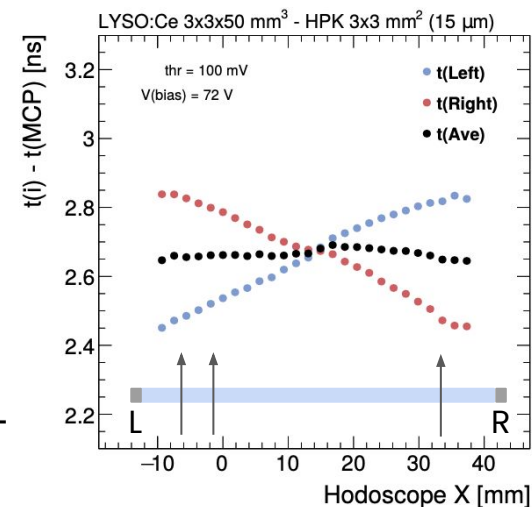
- **High aspect-ratio geometry**

- exploit total internal reflection to enhance light collection
- minimize SiPM area / crystal area
 - smaller power consumption
 - better timing performance (higher S/N after irradiation)

- **Double-end readout:**

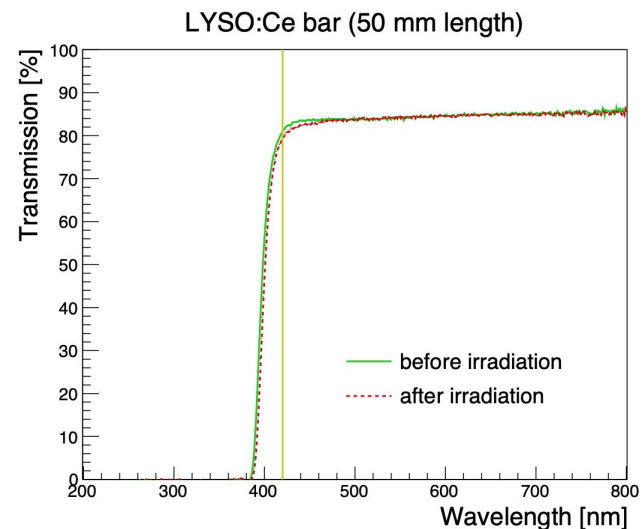
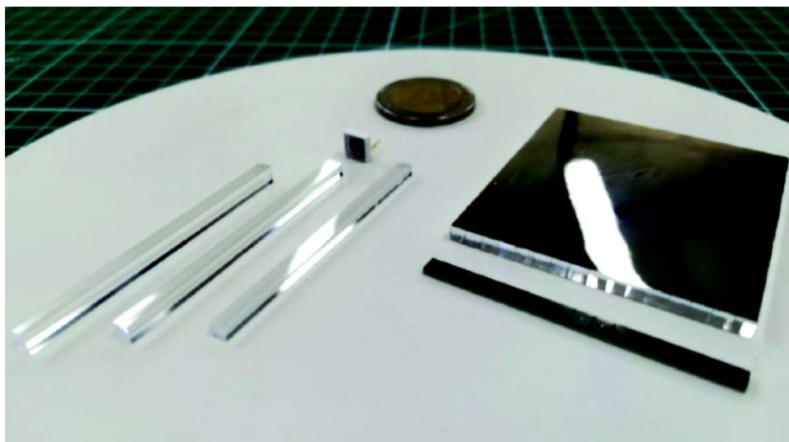
- improve resolution by $\sqrt{2}$ over single-end
- provides uniform response along the bar

$$t_{mip} = \frac{t_L + t_R}{2}$$



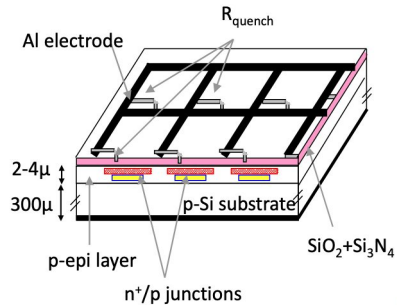
LYSO:Ce crystals as scintillator

- Well established technology (PET)
- Fast scintillation kinetics: $\tau_{\text{rise}} \sim 100$ ps, $\tau_{\text{decay}} \sim 40$ ns
- Dense (> 7.1 g/cm³), high Light Yield: 40000 γ /MeV \rightarrow large signals
- Radiation hardness proven up to 50 kGy and 3×10^{14} 1 MeV n_{eq} /cm²

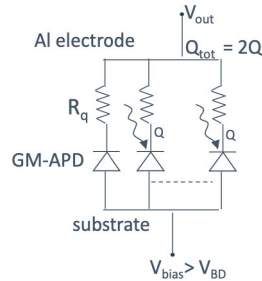


Silicon photomultipliers (SiPM) as photo-detectors

SiPM principle of operation



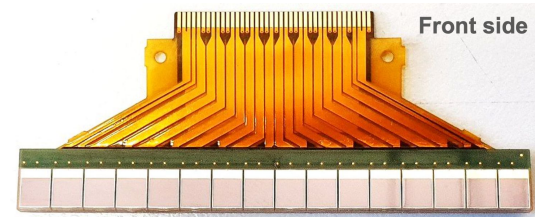
(FNIT-2011 CERN)



- A SiPM is an array of small cells (SPADs) connected in parallel on a common substrate and operated in Geiger mode, each with its own quenching resistor
- Each element is independent and gives the same signal when fired by a photon
- The output signal is the sum of the signals produced by the individual cells

SiPMs as photodetectors for CMS BTL

- compact, insensitive to magnetic field
- fast (single photon response time spread 100 ps) → crucial for timing
- high (20–50%) Photon Detection Efficiency at LYSO emission peak



array of 16 SiPMs for the CMS BTL

Major challenge: SiPM Dark Count Rate (DCR) increasing up to O(10) GHz after 3000 fb⁻¹ (2E14 n_{eq}/cm²) due to radiation damage

Contributions to the time resolution

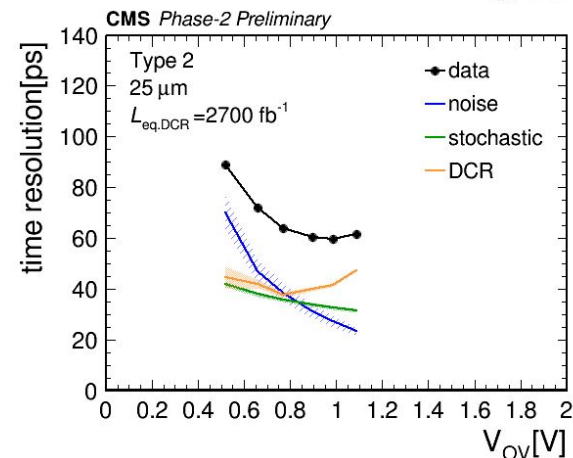
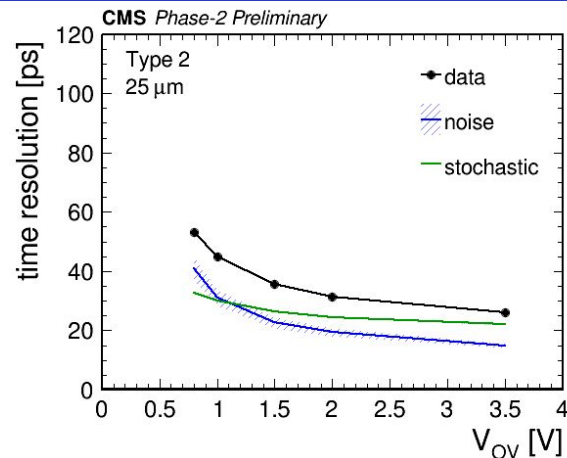
$$\sigma_t = \underbrace{\sigma_t^{phot} \oplus \sigma_t^{ele} \oplus \sigma_t^{DCR}}_{\text{dominant}} \oplus \underbrace{\sigma_t^{digi} \oplus \sigma_t^{clock}}_{\text{subdominant (< 15 ps)}}$$

- **photo-statistics:** $\sigma_t^{phot} \sim \frac{1}{\sqrt{N_{pe}}}$
- **electronics noise:** $\sigma_t^{ele} = \frac{\sigma_{noise}}{dV/dt} \sim \frac{\sigma_{noise}}{gain \cdot N_{pe}}$
- **radiation induced DCR noise:** $\sigma_t^{DCR} \sim \frac{\sqrt{DCR}}{N_{pe}}$
→ dominant at end of operation!

Time resolution driven by photon signal (N_{pe}), radiation induced dark counts (DCR) and electronic signal rising slope (dV/dt)

$$N_{pe} = \underbrace{LY}_{\text{crystals}} \cdot \underbrace{Edep}_{\text{crystals + SiPMs}} \cdot \underbrace{LCE}_{\text{crystals + SiPMs}} \cdot \underbrace{PDE}_{\text{SiPMs}}$$

Edep: energy deposited by the MIP
LY: crystal light yield
LCE: light collection efficiency
PDE: photon detection efficiency

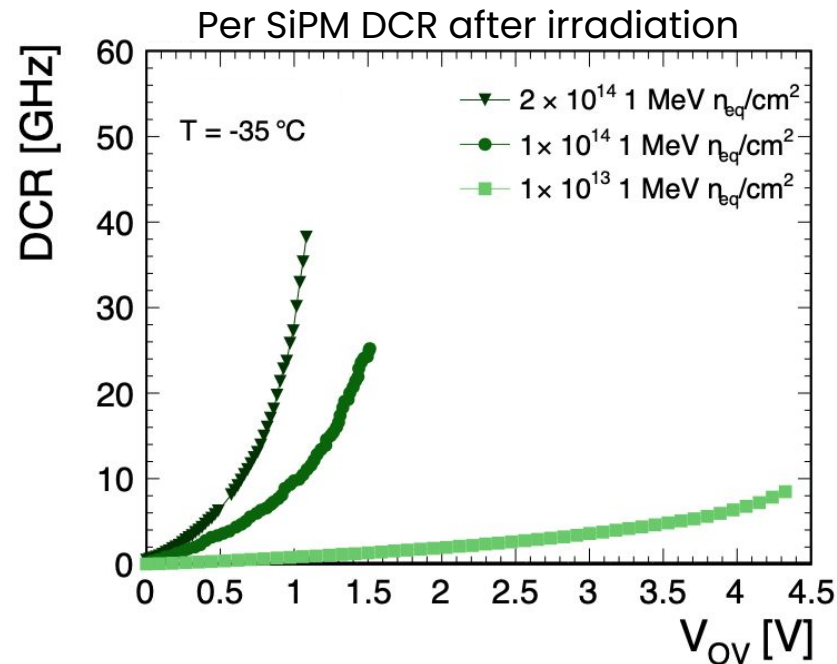


Solutions to deal with the SiPM dark noise

Radiation induced DCR noise is the dominant term contributing to the time resolution of irradiated SiPMs.

Solutions adopted to deal with DCR:

- **Smart thermal management:**
SiPM operation at cold temperature and annealing at high temperature
- **Decrease of the SiPM operating voltage along detector lifetime**
- **Dedicated DCR noise filtering in the ASIC**
- **Optimization of the sensors: SiPM cell size and LYSO thickness**

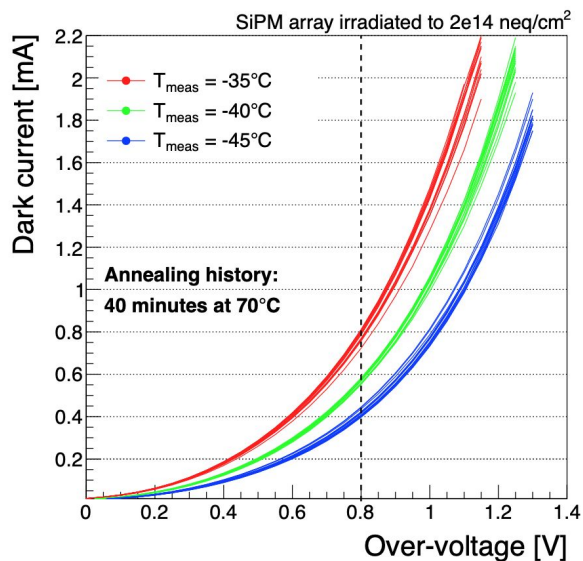


DCR: effect of temperature and annealing

DCR and SiPM operating temperature

**SiPM dark current reduced by factor ~2
for $\Delta T = -10^\circ\text{C}$**

Operating temperature is a powerful tool to reduce DCR and power consumption

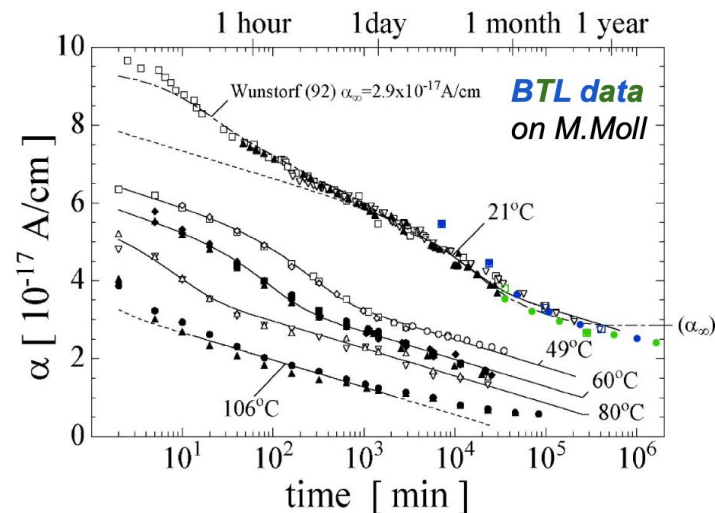


DCR and SiPM annealing

Radiation-induced defects in silicon anneal with a temperature dependent behavior [[M.Moll](#)]

$$\Delta I = \alpha \Phi V_d$$

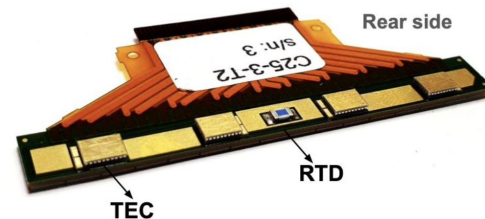
α = current-related damage constant
 Φ = fluence
 V_d = depletion volume



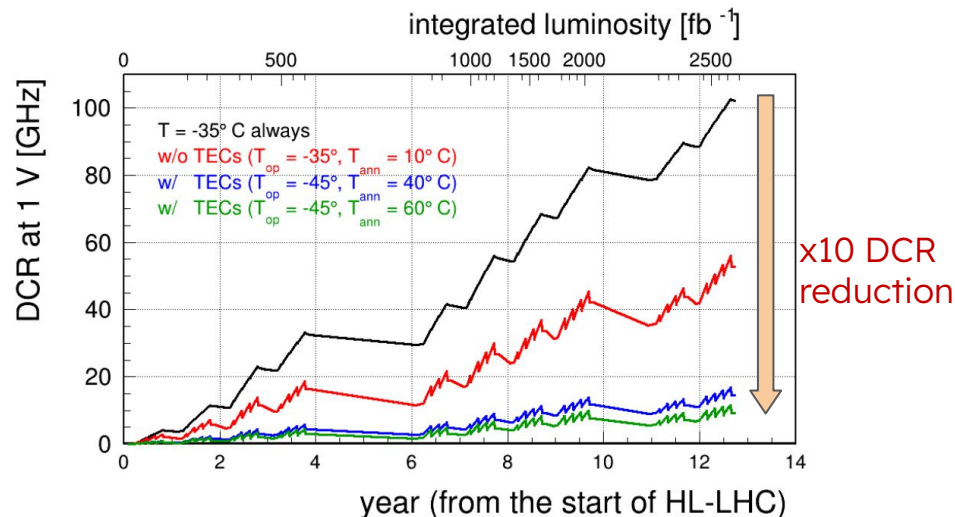
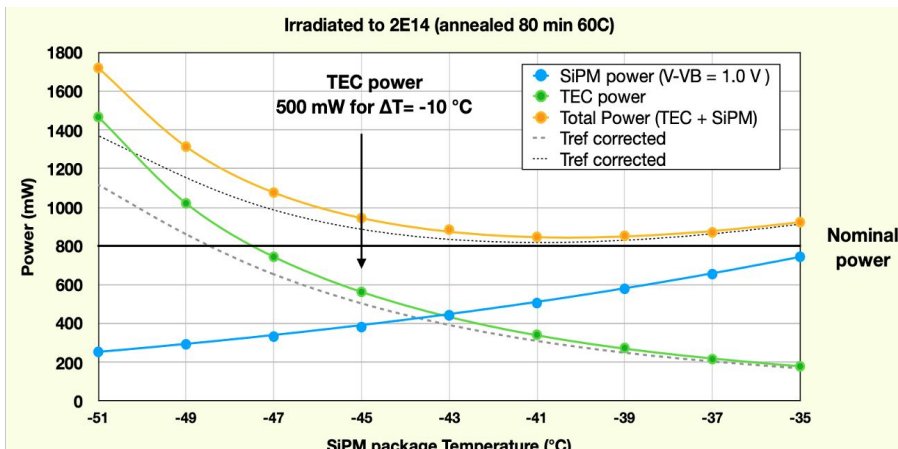
Smart thermal management

- CO₂ cooling at T = -35°C + additional cooling (→ **T_{op} = -45°C**) using mini Thermo-electric Coolers (TECs) integrated in the SiPM package
- in-situ **annealing cycles (T = +60°C)** during technical stops/machine shutdown (reverse TEC bias)
- **x10 DCR reduction** (wrt to the case of no TECs)

2023 JINST 18 P08020



Total power consumption for full array



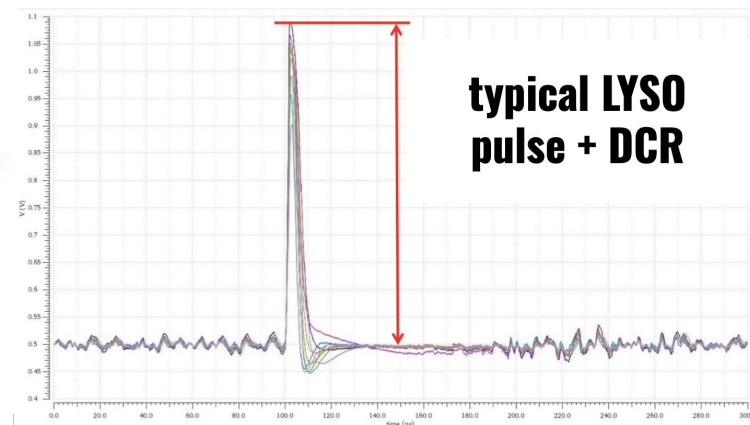
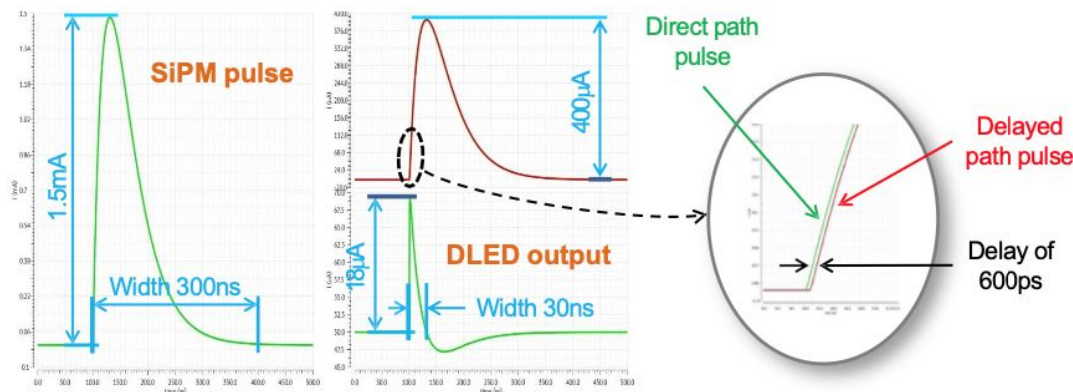
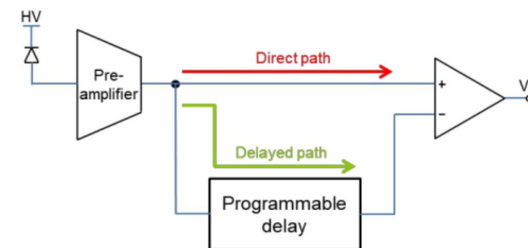
DCR noise filtering in the ASIC

- Differential leading-edge discrimination (DLED) in the TOFHIR2 ASIC
 - Inverted and delayed pulse added to the original pulse
 - Delay line approximated by a programmable RC network in the ASIC
 - the DCR noise is reduced (auto-correlated noise on the time scale of the single p.e. pulse)
 - fast rising edge of the signal (“early photoelectrons”) preserved

DLED signal processing

$$h[f(t)] = f(t) - f(t-\delta t)$$

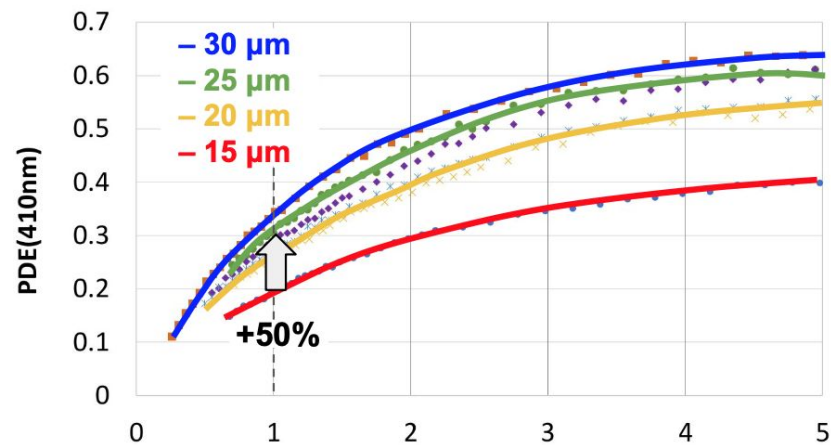
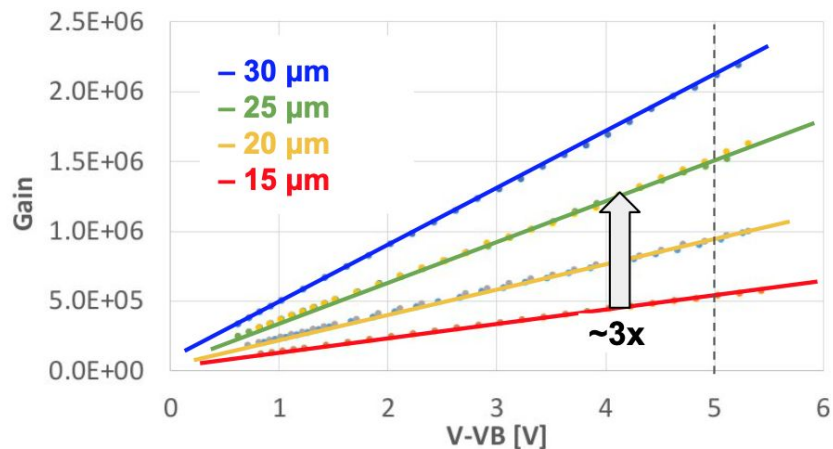
$$\delta t = [200 \ 800] \text{ps}$$



[2024 JINST 19 P05048](#)

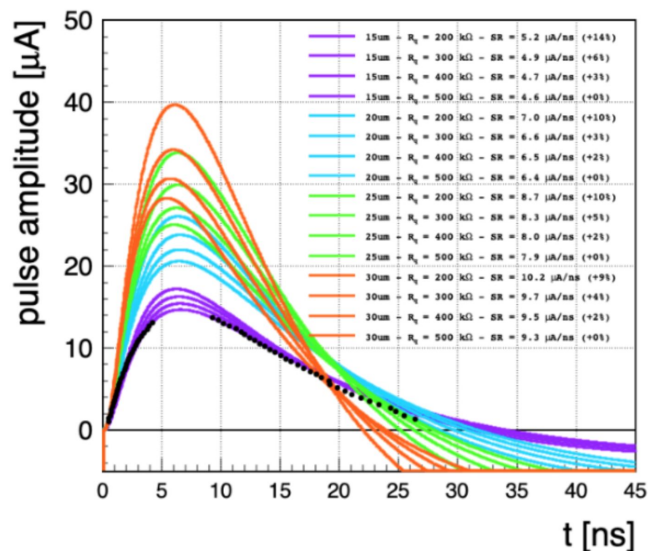
SiPM cell-size optimization

- **SiPM with larger cell size** have **larger PDE** (thanks to the higher fill factor and better cell depletion at low OV) and **higher gain**
 - → large signals!

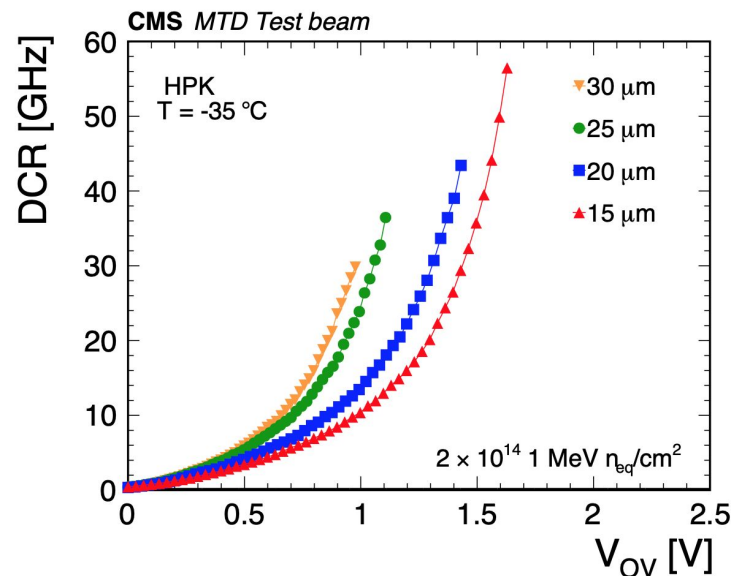


SiPM cell-size optimization

- **SiPM with larger cell size** have **larger PDE** (thanks to the higher fill factor and better cell depletion at low OV) and **higher gain**
 - → large signals!
- **Choice of the optimal SiPM micro-cell size is a trade-off between PDE/gain and DCR/power dissipation**
 - **DCR (as PDE) increases** with the SiPM effective active area



15 μm
20 μm
25 μm
30 μm



LYSO thickness optimization



- **Thicker crystals** → **larger energy deposit by the MIP**
→ **larger N_{pe} ($N_{pe} \propto \text{thickness}$)**
 - beneficial to all three terms of the time resolution
- But also larger DCR and power consumption because the SiPM active area is increased to match the crystal end face for optimal light collection
- DCR term (dominant after irradiation) scales $\sim \sqrt{\text{DCR}/N_{pe}} \sim 1/\sqrt{\text{thickness}}$

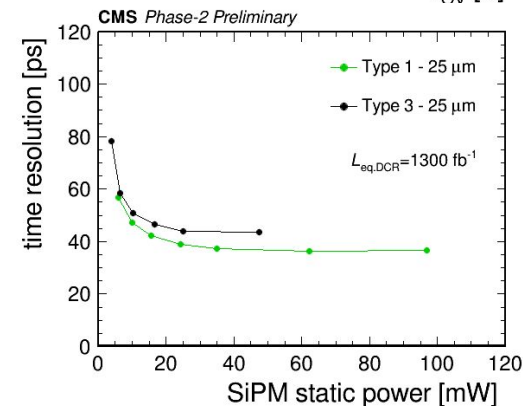
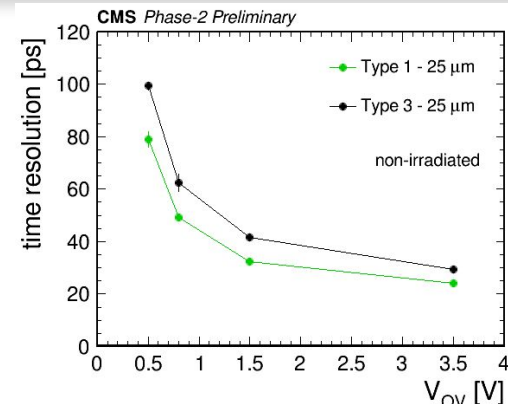
$$\sigma_t^{phot} \sim \frac{1}{\sqrt{N_{pe}}}$$

$$\sigma_t^{ele} = \frac{\sigma_{noise}}{dV/dt} \sim \frac{\sigma_{noise}}{gain \cdot N_{pe}}$$

$$\sigma_t^{DCR} \sim \frac{\sqrt{DCR}}{N_{pe}}$$

Thicker crystals remain beneficial also for after irradiation despite the larger DCR

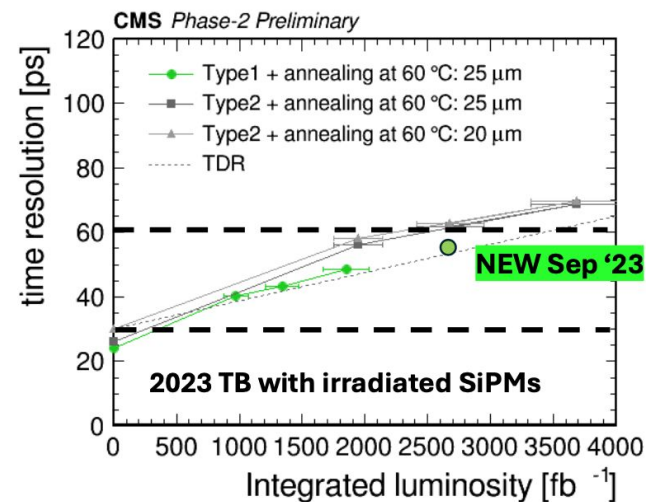
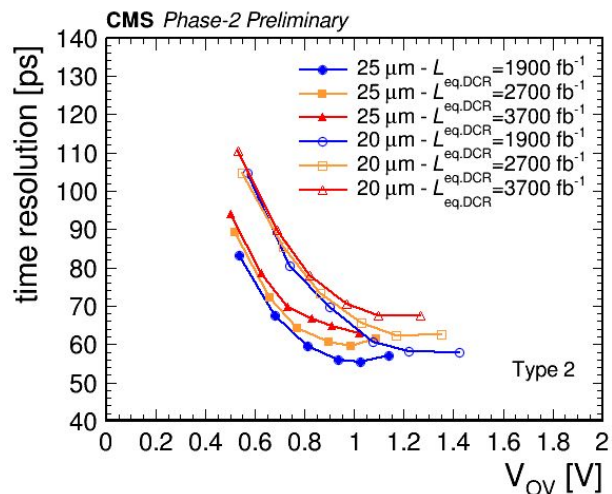
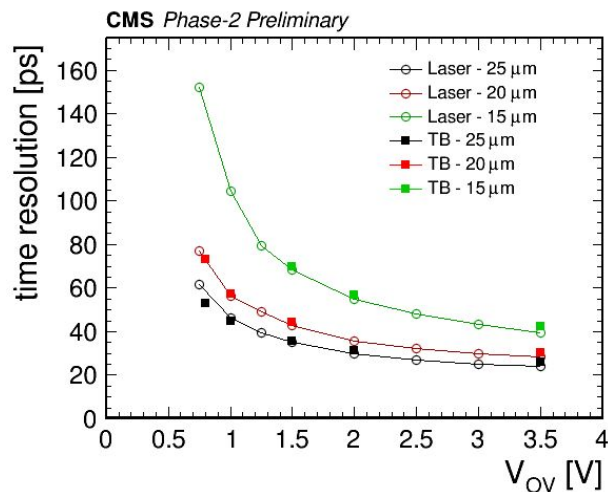
Confirmed with test beam data



BTL performance

- The performance of BTL module prototypes with both non-irradiated SiPM and irradiated to the total radiation level expected at end of operation was validated through beam and laboratory measurements
- Achieved
 - **30 ps** for HL-LHC beginning of operation
 - **~ 60 ps** for HL-LHC end of operation

25 μm SiPMs + thick LYSO identified as the optimal configuration for BTL

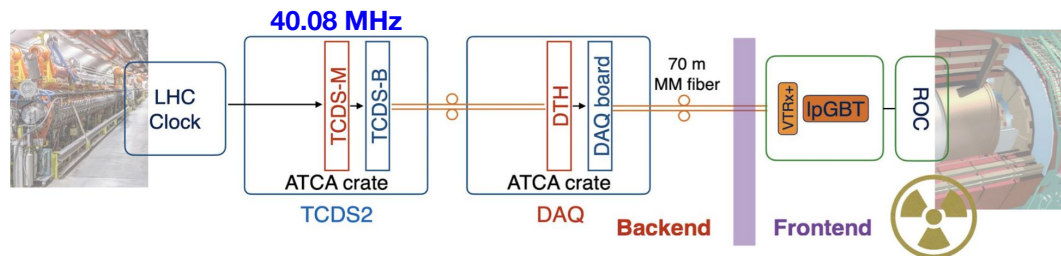


System aspects

- Clock distribution
- Channel cross-calibration

System aspects: clock distribution

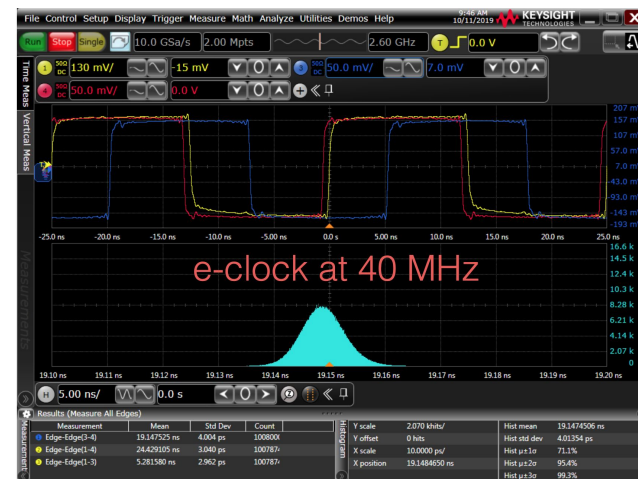
- Clock distribution crate should provide a stable clock with less than 15 ps RMS jitter



- The precision clock is synchronized to the LHC bunch frequency (40MHz) and is received by the subsystem and transmitted to the detector via high-speed data links.

$$\sigma_t^2 = \sigma_{jitter}^2 + \sigma_{ioniz.}^2 + \sigma_{TDC}^2 + \sigma_{clock}^2$$

Front-end retrieves clock phase and fans out the clock to $>10^5$ channels

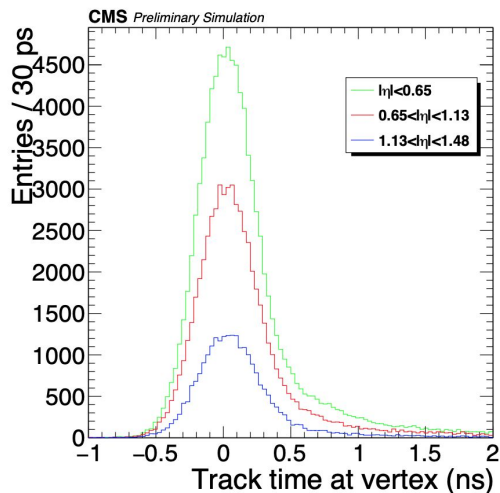


Clock test display with full chain: **RMS jitter ~ 4 ps**

System aspects: cross calibration

Time alignment

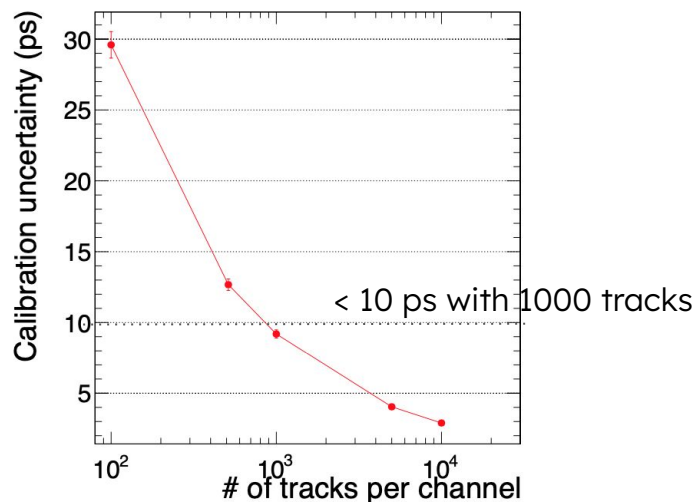
- Different clock paths (fiber/cable lengths) across the systems generates relative time offsets
- Time offsets can be calibrated by aligning the measurements of the time of arrival of track from the collision vertex



Time at vertex through track-fit back propagation independent of pseudorapidity

Cross calibration precision

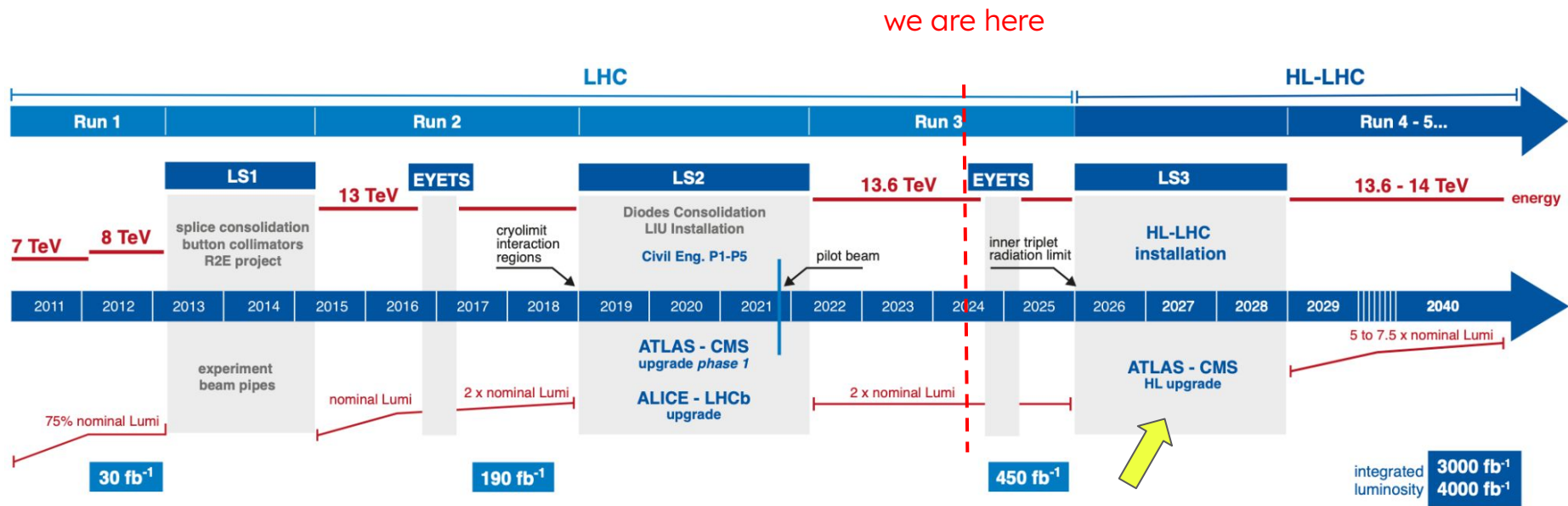
- Beam spot spread 200 ps
- Uncertainty on the mean: $200 \text{ ps} / \sqrt{N}$



1000 tracks can be collected in ~20 s per channel → possibility of frequent granular monitoring and calibration

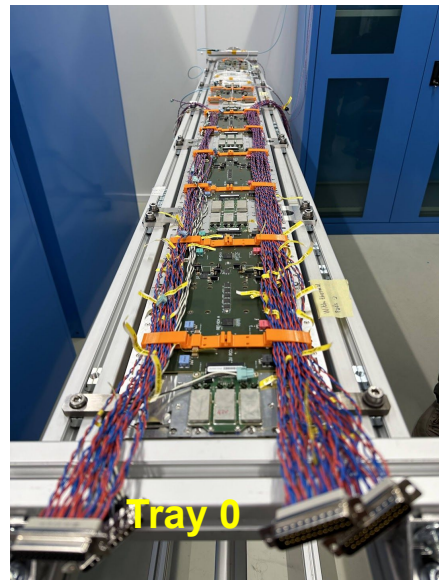
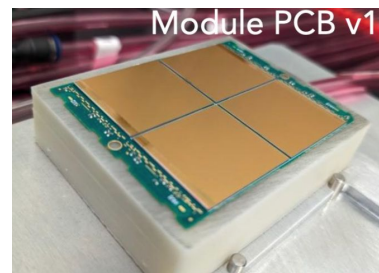
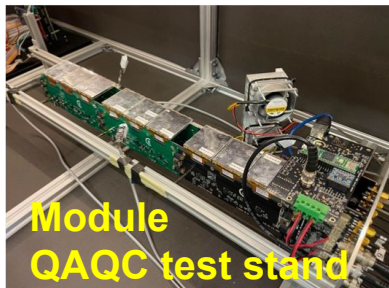
Schedule

LHC schedule



- CMS BTL to be installed at the beginning of LHC long shutdown (LS3), before the CMS tracker → **starting assembly in summer 2024!**

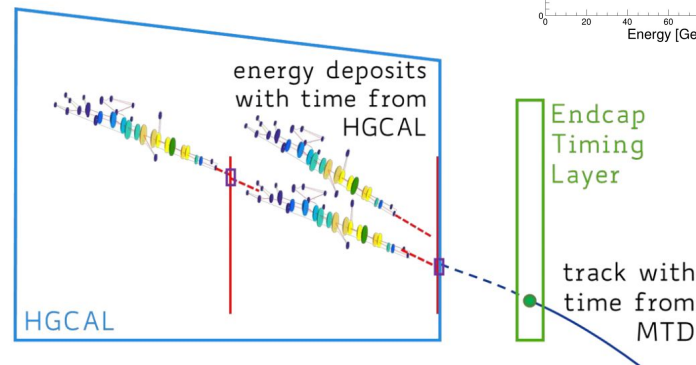
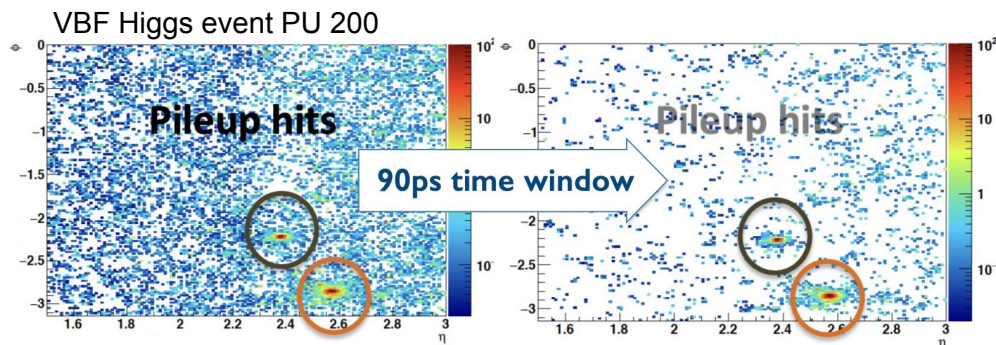
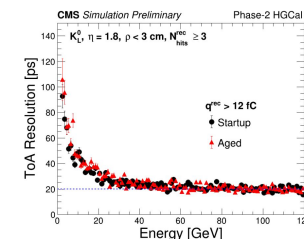
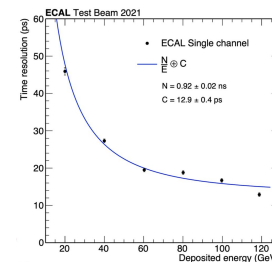
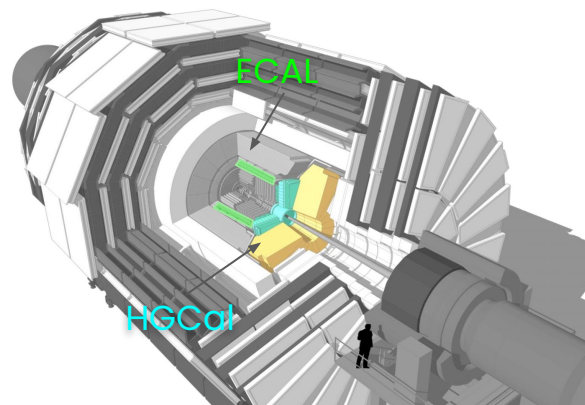
Where we are?



Extra: timing in the CMS upgraded calorimeters

Precision timing also in the CMS calorimeters!

- **CMS ECAL Barrel**
 - PbWO_4 + APDs
 - upgrade of the electronics
 - $\sigma_t \sim 30$ ps for showers $E > 50$ GeV
- **CMS High Granularity Calorimeter (HGCAL)**
 - Silicon sensors + absorbers (Pb, CuW, Cu)
 - $\sigma_t < 30$ ps for clusters $E > 5$ GeV



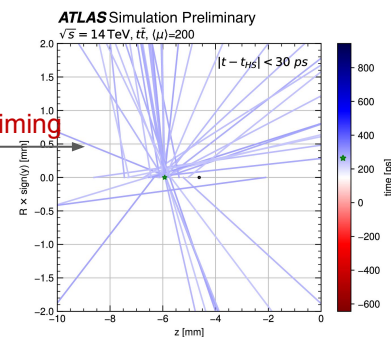
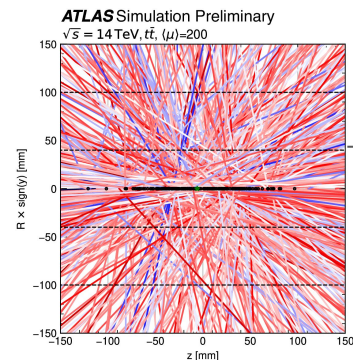
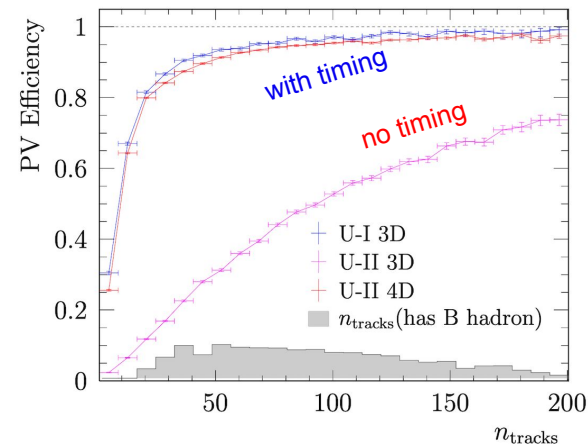
Timing from MTD + calorimeters → **towards a time-aware global event description**

Applications of precision timing in future detectors

- Use cases: 4D tracking/vertex timing, TOF measurements for PID, calorimetry

4D tracking/vertex timing

- **LHCb detector upgrade II** after LS4 LHC (~2035)
[[LHCb-TDR-023](#)]
 - plan upgrade of the Vertex Locator
 - timing at 50 ps/hit allows recovering primary vertex finding efficiency
 - explored different technologies, 3D Si sensors as baseline
- ATLAS also investigating physics impact of 4D tracking in the *central* part beyond LHC Run4
[[ATL-PHYS-PUB-2023-023](#)]
- **Future hadron colliders (FCC-hh)**
 - Unprecedented $O(1000)$ pileup conditions
 - Clear case for the use of 4D technology in tracking layers
 - Associate hits consistent in time
 - Need 5-10ps resolution per track
 - Dedicated R&D required to archive a radiation hardness for an intensity 30 times larger than HL-LHC



TOF measurements for PID

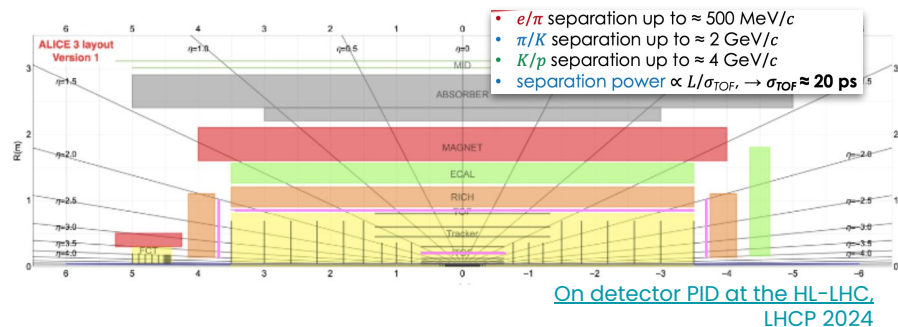
- **Heavy ions physics -**

- **ALICE 3 upgrade after LS4 LHC:**

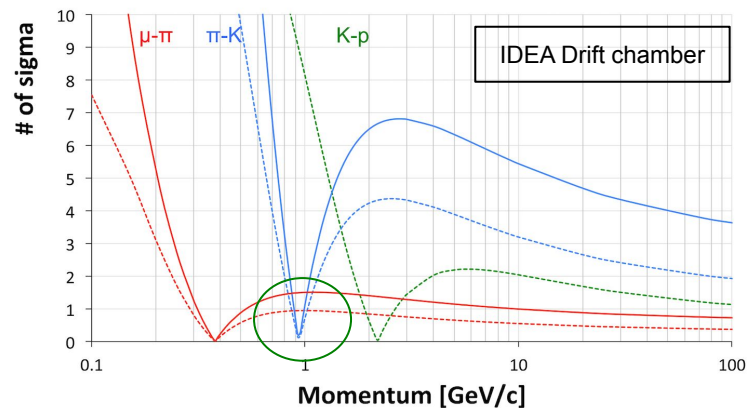
- TOF system with 20 ps resolution for PID of intermediate momentum particles
- different Si-based technologies under investigation (LGADs, CMOS, SiPMs)

- **Hadron identification for flavour physics at future colliders e+e-**

- PID largely relies on dE/dx and Cherenkov
- A TOF detector with $O(100)$ ps resolution at 2 m (outer tracker radius) could cover the π -K "cross-over" region at ~ 1 GeV, where dE/dx is blind
- Moreover, with TOF
 - redundant π/K separation up to ~ 5 GeV
 - vertex timing ($\sigma_{\text{Vtx}} \sim \sigma_{\text{TOF}} / \sqrt{N_{\text{tracks}}}$)



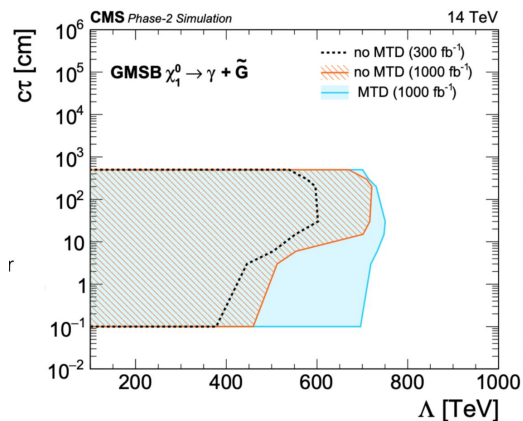
Particle Separation (dE/dx vs dN/dx)



Timing in calorimetry

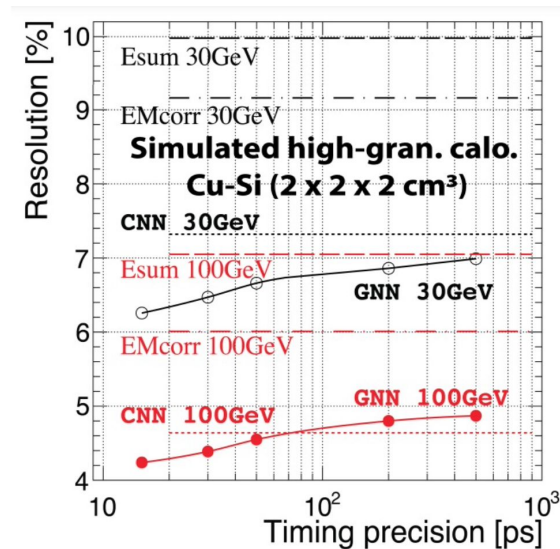
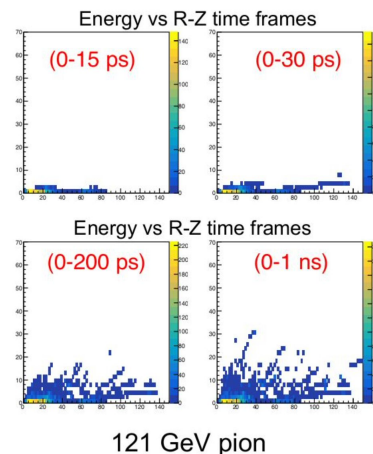
Timing of neutral particles

- example: HL-LHC with 30 ps resolution for photons
- LLP searches with neutrals: sensitivity at short $c\tau$ limited by timing resolution, with dominant contributions from:
 - beam spot size w/o vertex timing
 - shower time resolution w/ vertex timing



Adding timing information in hadron shower reconstruction (timing within the shower)

- can improve resolution and linearity



[N. Akchurin et al, Calor2022](#)

- **Precision timing is expected to assume a pivotal role in HL-LHC, offering a solution to mitigate the expected high levels of pileup and enabling new physics opportunities**
- **Unprecedented challenges posed by the harsh radiation environment of the HL-LHC require smart solutions, extensive R&D and prototyping**
- **Different sensor technologies adopted to meet the design target:**
 - silicon based sensors (**LGADs**) for the CMS ETL and ATLAS HGDT
 - light detectors (**LYSO+SiPM readout**) for the CMS BTL
- **The development and construction of MIP timing detectors at the LHC represent a pioneering effort towards usage of precision timing future collider-based particle physics experiments**